Title
An examination of chemistry and transport processes in the tropical lower stratosphere using observations of long-lived and short-lived compounds obtained during STRAT and POLARIS

Journal
Journal of Geophysical Research Atmospheres, 104(D21)

ISSN
0148-0227

Authors
Flocke, F
Herman, RL
Salawitch, RJ
et al.

Publication Date
1999-11-20

DOI
10.1029/1999JD900504

JOURNAL OF GEOPHYSICAL RESEARCH, VOL. 104, NO. D21, PAGES 26,625-26,642, NOVEMBER 20, 1999

An examination of chemistry and transport processes in the tropical lower stratosphere using observations of long-lived and short-lived compounds obtained during STRAT and POLARIS

F. Flocke,[1] R. L. Herman,[2] R. J. Salawitch,[2] E. Atlas,[1] C. R. Webster,[2] S. M.Schauffler,[1] R. A. Lueb,[1] R. D. May,[2] E. J. Moyer,[3] K. H. Rosenlof,[4] D. C. Scott,[2] D. R. Blake,[5] and T. P. Bui[6]

Abstract. A suite of compounds with a wide range of photochemical lifetimes (3 months to several decades) was measured in the tropical and midlatitude upper troposphere and lower stratosphere during the Stratospheric Tracers of Atmospheric Transport (STRAT) experiment (fall 1995 and winter, summer, and fall 1996) and the Photochemistry of Ozone Loss in the Arctic Region in Summer (POLARIS) deployment in late summer 1997. These species include various chlorofluorocarbons, hydrocarbons, halocarbons, and halons measured in whole air samples and CO measured in situ by tunable diode laser spectroscopy. Mixing ratio profiles of long-lived species in the tropical lower stratosphere are examined using a one-dimensional (1-D) photochemical model that includes entrainment from the extratropical stratosphere and is constrained by measured concentrations of OH. Profiles of tracers found using the 1-D model agree well with all the observed tropical profiles for an entrainment time scale of 8.5^{+6}_{-4} months, independent of altitude between potential temperatures of 370 and 500 K. The tropical profile of CO is used to show that the annually averaged ascent rate profile, on the basis of a set of radiative heating calculations, is accurate to approximately ±44%, a smaller uncertainty than found by considering the uncertainties in the radiative model and its inputs. Tropical profiles of ethane and C_2Cl_4 reveal that the concentration of Cl is higher than expected on the basis of photochemical model simulations using standard gas phase kinetics and established relationships between total inorganic chlorine and CFC-11. Our observations suggest that short-lived organic chlorinated compounds and HCl carried across the tropical tropopause may provide an important source of inorganic chlorine to the tropical lower stratosphere that has been largely unappreciated in previous studies. The entrainment timescale found here is considerably less than the value found by a similar study that focused on observations obtained in the lower stratosphere during 1994. Several possible explanations for this difference are discussed.

1. Introduction

Dynamical processes in the tropical lower stratosphere can have an important impact on the physical and chemical processes that, for example, influence radiative forcing, heating budgets, and ozone photochemistry [e.g., *Holton et al.*, 1995, and references therein]. Tracer observations obtained in the tropical stratosphere suggest a strong degree of isolation of the region of large-scale tropical ascent (roughly, within 15° of the equator) from the midlatitude stratosphere [e.g., *Boering et al.*, 1994, 1996; *Mote et al.*, 1996; *Murphy et al.*, 1993; *Randel et al.*, 1993; *Trepte and Hitchman*, 1992; *Wofsy et al.*, 1994]. To address these observations, *Plumb* [1996] developed the "tropical pipe" model of stratospheric circulation, which essentially isolates air in the tropical upwelling region from air at midlatitudes. However, it has been shown that a limited amount of irreversible mixing must occur between midlatitude and tropical air in the lower stratosphere to accurately describe the tracer observations obtained in the tropics [e.g., *Avallone and Prather*, 1996; *Hall and Waugh*, 1997; *Herman et al.*, 1998; *Minschwaner et al.*, 1996; *Mote et al.*, 1998; *Schoeberl et al*, 1997; *Volk et al.*, 1996]. Emphasis has been placed recently on quantifying the characteristic "entrainment time" for irreversible mixing of midlatitude stratospheric air into the tropical stratosphere, because this mixing process plays an important role in the redistribution to higher altitudes of pollutants released at midlatitudes, in particular, with respect to a proposed fleet of supersonic aircraft [*Stolarski*, 1995]. Previous studies have suggested that entrainment is fastest below 20 km [e.g., *Herman et al.*, 1998; *Minschwaner et al.*, 1996; *Mote et al*, 1998; *Schoeberl et al.*, 1997], but this conclusion has been limited by large uncertainties related to the calculated ascent rate in the tropics as well as the use of tracers with photochemical lifetimes too long so that key assumptions could not be tested. This study

[1]NCAR Atmospheric Chemistry Division, Boulder, Colorado.
[2]NASA Jet Propulsion Laboratory, California Institute of Technology, Pasadena.
[3]Division of Geological and Planetary Sciences, California Institute of Technology, Pasadena
[4]NOAA Aeronomy Laboratory, Boulder, Colorado.
[5]Department of Chemistry, University of California at Irvine.
[6]NASA Ames Research Center, Moffett Field, California.

Paper number 1999JD900504
0148-0227/99/1999JD900504$09.00

uses a unique set of tracer observations obtained during the Stratospheric Tracers of Atmospheric Transport (STRAT) and Photochemistry of Ozone Loss in the Arctic Region in Summer (POLARIS) missions on board the NASA ER-2 aircraft [*Newman et al.*, this issue] by the Whole Air Sampler (WAS) and the Aircraft Laser Infrared Absorption Spectrometer (ALIAS). The suite of tracers analyzed here covers a range of local photochemical lifetimes between 3 months and several hundred years.

We use a one-dimensional (1-D) photochemical transport model to simulate the altitude profiles of the volume mixing ratios (referred to as "vmr profile" below) of tracers observed at altitudes between 16 and 20.5 km in the tropics [*Herman et al.*, 1998]. Because of the limited number of tracer data, we do not treat seasonal variations in this model. Instead, our results reflect the mean stratospheric transport averaged over a 2-year period (mid-1995 to mid-1997). Since the abundances of many of the species are strongly influenced by various chemical loss processes, the photochemistry applied in the model needs to be realistic. We use both a photochemical steady state model of the lower stratosphere and in situ observations of radicals made on board the ER-2 to estimate photochemical removal rates. Reaction with chlorine radicals is the primary sink for several short-lived species (i.e., ethane and C_2Cl_4) and an important loss process for methane throughout the lower stratosphere. Therefore we use measured ethane and C_2Cl_4 vmr profiles to obtain an independent estimate of the vmr profile of atomic chlorine in the tropical lower stratosphere that we believe is more realistic than values of Cl found using a photochemical model, owing mainly to uncertainties in Cl_y. The CO vmr profile is used to constrain the ascent rate profile. The vmr profiles of the long- and medium-lived species are then used to constrain the average entrainment timescale. Finally, we compare our results to earlier studies and discuss possible implications.

2. Experiment

2.1. Whole Air Sampler

The main component of WAS is a set of 29-49 specially treated stainless steel canisters that are filled with ambient air to a pressure of about 3000 hPa in flight by means of an all-metal bellows pump [*Heidt et al.*, 1989]. The filling time varies with flight altitude between less than 10 s in the upper troposphere to about 200 s at 21 km. During three of the tropical flights we programmed the WAS to acquire samples with the highest possible frequency to achieve good altitude coverage, that is, about 20-25 samples per dive. The canisters are transported back to the National Center for Atmospheric Research (NCAR) and analyzed in the laboratory. About 50 different species, including CFCs, HCFCs, HFCs, halons, other halogenated compounds, and alkyl nitrates, are quantified by gas chromatography-mass spectrometry (GC-MS) (HP 5890/5971), operated in single-ion mode. The mixing ratios of methane (CH_4) and light hydrocarbons (C_2 to C_4) are measured using gas chromatography-flame ionization detection (GC-FID) (HP 5890). The limit of detection (LOD) for the nonmethane hydrocarbons is about 2 parts per trillion by volume (pptv), and the precision of the measurement is better than 2% or 2 pptv. In the case of the GC-MS instrument, LODs for the different species vary because of different specific responses and background noise for the quantitation ions used but are generally better than 0.1 pptv. The measurement accuracy also varies because of different individual relative responses, but an overall estimate of better than 5% or the LOD (whichever is larger) can be made. More details about our analytical procedures, canister preparation, etc. are given by *Daniel et al.* [1996], *Flocke et al.* [1998], and *Schauffler et al.* [1999]. We note that, specifically for the short-lived species, the accuracy of our measurements can be limited by variable background concentrations of these substances in the canisters (caused by outgassing of the sampling lines, the manifold system, or the canister walls) rather than by the LOD of the analytical instrument. We will discuss these background issues and their effect on the model analyses later in the paper.

2.2. Aircraft Laser Infrared Absorption Spectrometer

ALIAS is a high-resolution, midinfrared absorption spectrometer using four tunable diode lasers (TDLs) to simultaneously measure the concentration of CO, N_2O, CH_4, and HCl. Ambient air is drawn into a Herriott cell with a light path of 80 m and a flush time of less than 2 s. The system has been described in detail by *May and Webster* [1993] and *Webster et al.* [1994]. For CO the instrument precision (±1 standard deviation) is ±0.7 parts per billion by volume (ppbv) for a 3-s average value. The estimated instrument accuracy (±1 standard deviation) is ±5% relative to the calibration standards supplied by the National Oceanic and Atmospheric Administration's (NOAA) Climate Monitoring and Diagnostics Laboratory (CMDL).

2.3. Harvard HO_x Instrument

The concentration of the hydroxyl radical (OH) is a critical parameter for our model calculations. In situ measurements of OH and HO_2 were made on board the ER-2 by the Harvard HO_x instrument. The instrument is based on UV laser-induced fluorescence and is described by *Wennberg et al.* [1994a]. The accuracy and precision of the OH measurement are stated to be ±25% and ±0.10 pptv, respectively. The measured OH concentration is a strong function of solar zenith angle [e.g., *Salawitch et al.*, 1994; *Wennberg et al.*, 1994b] but is relatively independent of altitude in the tropical lower stratosphere [*Herman et al.* 1999]. *Herman et al.* [1999] used a quadratic fit of the observed concentration of OH as a function of solar zenith angle to obtain an annual, 24-hour mean concentration of $8\pm3\times10^5$ cm^{-3} for the tropical lower stratosphere. All subsequent chemical calculations are performed using this value for the concentration of OH.

2.4. Meteorological Parameters

Temperature and pressure were obtained from in situ measurements made by the ER-2 Meteorological Measurement System (MMS), which is described in detail by *Scott et al.* [1990]. Stated uncertainties in the measurements of temperature and pressure have no discernible impact on the analysis presented here.

2.5. Flights

Data were analyzed for six equatorial survey flights of the ER-2, going south from Barbers Point Naval Air Station, Oahu (21°N, 158°W), to about 3°S latitude along (±5°) the 160°W meridian. Measurements of the NO_y/O_3 ratio [*Murphy et al.*, 1993] confirm that tropical air was sampled during periods of each of these flights (see below). Five of these flights were performed during the STRAT program on November 5, 1995

(referred to as 951105), and on February 13, August 1, August 8, and December 11, 1996 (960213, 960801, 960808, and 961211, respectively). One flight was performed during POLARIS on September 23, 1997 (970923). All instruments reported data for each flight except that the WAS did not fly on 951105. Tracer concentration profiles at midlatitudes were obtained from stair-step flights and ascents/descents of the ER-2 out of NASA Ames Research Center (ARC)(37.4°N, 122.0°W) during numerous STRAT and POLARIS flights from all seven deployments of the ER-2 (October-November 1995 (CO only); January-February, July-August, September (CO only), and December 1996; April-May, June-July, and September 1997). In addition, we used results from canister analyses of samples collected by the WAS in the upper troposphere during the Pacific Exploratory Mission (PEM)-Tropics mission [*Hoell et al.*, 1999; *Schauffler et al.*, 1999, E. Atlas et al., Observations of marine alkyl nitrate emissions in the Pacific during PEM-Tropics, manuscript in preparation, 1999] on board the NASA DC-8 and P3B aircraft in late summer 1996 to infer the interhemispheric gradients of the tracers' mixing ratios (see below).

3. Model

3.1. Approach

We simulate vertical profiles of measured tracers in the tropical lower stratosphere using a one-dimensional model that includes vertical advection, horizontal entrainment of extratropical air, and full photochemistry for each species. The model assumes that the tropical mixing ratio χ of each tracer is controlled by local photochemical production and loss as well as by mixing with air parcels entrained from the extratropics. This approach is similar to those of Volk et al. [1996] and *Minschwaner et al.* [1996]. The mixing ratio χ of a species with a local lifetime to photochemical loss τ_{chem} and a production term P is described by

$$Q\frac{\partial \chi}{\partial \theta} = P - \frac{\chi}{\tau_{chem}} - \left(\frac{\chi - \chi_{ML}}{\tau_e}\right) - \gamma\chi, \qquad (1)$$

where θ is the potential temperature, Q is the tropical net diabatic heating rate, χ_{ML} is the mixing ratio of the species at midlatitudes (at the same θ -level as χ), τ_e is the mean characteristic time for the entrainment of extratropical air, and $\gamma\chi$ is a term to account for the mean tropospheric growth rate of the species (averaged over the 1994-1997 time period for our data):

$$\gamma = \frac{\partial \chi_{trop}}{\partial t}(\chi_{trop})^{-1}, \qquad (2)$$

where χ_{trop} is the mean tropospheric mixing ratio. We assume that mixing occurs only along isentropic surfaces, that the tropical air sampled is representative of the large-scale ascent region (i.e., horizontal homogeneity in the tropics for the time of the observation), and that the extratropical air is described by an average altitude profile for each species (based on observations) which is representative of midlatitudes and unaffected by the mixing process. Equation (1) is solved for $\chi(\theta)$ to calculate profiles of the tropical mixing ratio of each species for various assumptions regarding τ_e, τ_{chem}, Q, P (considered only for CO), and χ_{ML}. The entrainment timescale τ_e is determined on the basis of the similarity of modeled and measured profiles in the tropics for the suite of tracers. We show in section 5 that uncertainties in the midlatitude tracer profiles, χ_{ML}, have the largest effect of any input model parameter on the derived value of τ_e.

Unlike the approach of *Volk et al.* [1996], we use our model to simulate the observed vmr profiles rather than using tracer-tracer correlations to infer τ_e. Our approach does not eliminate the need to use calculated mean heating rates to estimate τ_e but does provide the opportunity to establish whether a unique set of ascent rates, entrainment timescales, and chemical conditions can be found that fit all the observed vmr profiles of a large number of tracers. The unique contribution of this paper is the use of short-lived species, that is, CO to constrain ascent rates and ethane and C_2Cl_4 to constrain Cl concentrations, which improves the accuracy of the entrainment timescales estimated from the observed distributions of the long-lived species.

3.2. Photochemical Steady State Model

The photochemical loss terms required for (1) involving photolysis and reactions with O^1D or Cl were generated using the photochemical steady state (PSS) model described by *Salawitch et al.* [1994]. All reaction rates and photolysis cross sections necessary are from *DeMore et al.* [1997], unless noted otherwise. Photolysis rates and quantum yields for CH_3Cl, CFC-11, CFC-12, CFC-113, CFC-114, H-1211, H-2402, C_2Cl_4, and CH_3Br are obtained from a recent review by *Roeth et al.* [1998]. A recently measured rate coefficient for the reaction of tetrachloroethene (C_2Cl_4) with OH (R. Talukdar, private communication, 1998) is used.

Twenty-four-hour mean photolysis rates for the measured tracers are generated from actinic flux calculations at each potential temperature level of the 1-D model (see below) and for variations in solar zenith angle corresponding to 15-min increments throughout the day (e.g., 97 PSS model time intervals per day). To estimate annual mean tropical loss rates, the PSS model is run for equinox, summer solstice, and winter solstice solar illumination at 7°S, keeping O_3 and tracer profiles fixed at their mean tropical values. The model loss terms from each season are then averaged together (equinox × 2). The PSS model is constrained by the mean tropical profiles of O_3 and temperature obtained by the ER-2 and ozone mapping spectrometer (OMS) balloon platforms [*Herman et al.* 1998] between 0 and 30 km and by a climatology based on satellite observations [*Minschwaner et al.*, 1993; *Keating and Young*, 1985; updated by G.M. Keating, private communication, 1994] for altitudes between 30 and 80 km. The total column abundance of O_3 corresponding to model profiles of O_3 derived in this manner typically agrees with total O_3 measurements obtained by the Total Ozone Mapping Spectrometer (TOMS) satellite to within 5 Dobson units (DU) for specific times and locations of tropical flights of the OMS package. Model input profiles of CH_4, H_2O, CO, ethane, NO_y, total inorganic chlorine (Cl_y), and aerosol surface area (necessary to calculate concentrations of Cl and O^1D) are derived from ER-2 observations in the tropics.

The 24-hour mean concentration of OH based on in situ observations is used in the 1-D model described below owing to discrepancies between theory and observation of OH that are not completely resolved [e.g., *Herman et al.*, 1999]. The calculated OH tends to agree with observation to better than 15% near 20 km, with greater discrepancy (the modeled OH is less than measured OH, by as much as a factor of 2) at lower altitudes. This discrepancy is consistent with the tendency of the model, using measured NO_y, to underestimate observed NO (*see Osterman et al.* [1999] and *Gao et al.* [1999] for a discussion of a possible

Table 1. Simulated Tracers: Average Lifetimes, Main Loss Reactions, Interhemispheric Gradients, Average Growth Rates for the 1994-1997 Period, and Boundary Conditions for the 1-D Model

Species	Boundary Conc, pptv	Average Chemical Lifetime (at Theta Level), Years				Main Loss Process	Interhemispheric Gradient[a]	Growth Rate, s^{-1}
		370 K	420 K	470 K	500 K			
CO	5.8×10^{4}	0.26	0.26	0.27	0.27	OH	1	0
C_2Cl_4	0.40	0.33	0.06	0.05	0 05	Cl(0.89)[b], OH(0.11)[b]	1 40	0
C_2H_6	400	0.69	0.11	0.07	0.05	Cl(0.88)[b], OH(0.12)[b]	1.23	0
H-2402 (CF_2BrCF_2Br)	0.44	5.40	1.38	0.75	0.47	hν	1.08	$1\ 2\times10^{-9}$
H-1211 (CF_2ClBr)	3.42	7.00	1.63	0.87	0.54	hν	1.04	$1\ 1\times10^{-9}$
CH_3Br	9 50	7.43	2.22	1.21	0.77	OH	1.10	0
CH_3Cl	576	13.3	11.3	7.43	6.29	OH	1	0
CFC-11 ($CFCl_3$)	267	26.1	5.48	2.85	1.75	hν	1.01	-8.7×10^{-11}
CH_4	1.715×10^{6}	145	112	62 5	50.6	OH(0.78)[b], Cl(0.14)[b], O^1D (0 08)[b]	1.01	5.5×10^{-11}
	83	150	31 2	16.1	9 93	hν	1.01	4.8×10^{-10}
CFC-12 (CF_2Cl_2)	539	332	68.1	33.3	20.3	hν	1.01	$4\ 2\times10^{-10}$
CFC-114 (CF_2ClCF_2Cl)	14.0	1588	347	165	103	hν	1	3.0×10^{-10}

[1] Correction factor for the measured Northern Hemispheric average profiles between 370 and 420 K
[b] Relative importance at 410 K potential temperature level.

resolution to the discrepancy for stratospheric NO/NO_y). Constraining the model using measured NO improves the agreement with measured OH in the tropical lower stratosphere, but this calculation still tends to underestimate measured OH, particularly in the lowermost stratosphere. This discrepancy may indicate the influence of hydrogen radical precursors such as acetone or peroxides [*Singh et al.*, 1995; *Jaeglé et al.*, 1997; *Wennberg et al.*, 1998] that are unaccounted for in the model because they have not been measured in the tropical lower stratosphere. The observed concentration of OH in the tropics during the ER-2 flights described above exhibits a marked variation with solar zenith angle but little dependence on altitude for a fixed solar zenith angle [*Herman et al.*, 1999]. Consequently, for the 1-D model calculations described below, we use a value for the 24-hour mean concentration for OH of $8\pm3\times10^{5}$ cm^{-3}, independent of altitude and season, that was derived by *Herman et al.* [1999].

Carbon monoxide (CO) is the only tracer under consideration for which photochemical production is important. Production of CO from reactions of CH_4 with OH, O^1D, and Cl is calculated using measured profiles of CH_4, 24-hour mean concentration ~~profiles of O^1D~~ and Cl resulting from full diurnal PSS simulations for each potential temperature level and season, and the empirical 24-hour mean concentration of OH described above. Production of CO tends to be dominated by reaction of CH_4 with OH below about 480 K, with the reaction of CH_4 with Cl becoming important above this θ level (see Table 1).

The mixing ratio profile of Cl_y is an important and somewhat uncertain model input parameter. It is important because, to first order, the calculated concentration of Cl is linearly dependent on Cl_y. Reaction with Cl is the dominant loss process for ethane and C_2Cl_4 and the second most significant process for CH_4 loss and CO production in the stratosphere (see Table 1). Typically, vmr profiles for Cl_y used in photochemical models are generated from empirical relations between tropical measurements of the total chlorine content of the organic source molecules (CCl_y) and a tracer such as CFC-11, combined with the mean tropical vmr profile for CFC-11. As will be discussed below, Cl_y estimated in this manner for the tropical lower stratosphere is particularly uncertain because of the possible contribution of inorganic chlorine from the decomposition (in both the troposphere and stratosphere) of very short-lived organic compounds that are not typically considered in the definition of CCl_y. Various assumptions regarding model constraints for the vmr profile of Cl_y are considered, as described below.

We note that in situ observations of ClO obtained in the tropics for potential temperatures below 460 K on 970923 provide little constraint on calculated Cl. The measured vmr of ClO was below 15 pptv (near the detection limit) and displayed considerable scatter, with numerous individual 30-s average determinations lying below zero (R. Stimpfle et al., private communication, 1998). The large uncertainty in measured ClO cannot be used to rule out any of the various Cl profiles considered below. Finally, the in situ ClO instrument was not flown on any of the tropical ER-2 flights during the STRAT campaign. The observations of HCl, which provide a strong test of the model representation of inorganic chlorine partitioning when Cl_y is known accurately (e.g., at higher altitudes [*Sen et al.*, this issue]), are used here to better constrain our knowledge of Cl_y. This seems appropriate since $HCl \approx Cl_y$ for the conditions

(e.g., temperature, humidity, and aerosol surface area) of the tropical lower stratosphere using rates for heterogeneous reactions involving HCl given by *DeMore et al.* [1997].

3.3. One-Dimensional Model

As noted above, we simulate the 2-year mean vertical profiles of gases in the tropical lower stratosphere with a 1-D photochemical model described by (1). The diabatic heating rate Q is calculated using a model of infrared radiative transfer that is mass-balanced (e.g., constrained by zero net mass flux through a global pressure surface [*Rosenlof,* 1995]). The O_3 vmr profiles used in the radiative transfer model are inferred from UARS satellite observations. To obtain a representative profile of mean tropical heating rates, Q is averaged over deep tropical latitudes (9.5°S to 9.5°N), all longitudes, and both phases of the quasi-biennial oscillation (QBO) of stratospheric winds during the time of the ER-2 flights (July 1995 through June 1997). The 1-D model has 14 discrete levels equally spaced in log(pressure). The boundary condition for the mixing ratio of each species at the mean isentrope of the tropical tropopause, θ = 370 K, is derived from the tropical ER-2 and DC-8 flights. Equation (1) is numerically solved for $\chi(\theta)$ with Mathematica® (Wolfram Research, Champaign, Illinois), which uses cubic splines to interpolate between levels. The value of τ_e is varied (see below), and agreement with the measured tracer profiles is tested.

We have simulated the observed vmr profiles of a suite of 12 short- and long-lived tracers: CO, ethane, C_2Cl_4, CH_3Br, the halons H-1211 and H-2402, CH_3Cl, CFC-11, CFC-12, CFC-113, CFC-114, and CH_4. Table 1 lists for each compound the main loss process and the local photochemical lifetime at different potential temperature levels. The interhemispheric gradients and boundary conditions required for the 1-D model simulations (see below) are also given in Table 1. The tropical data were selected using the gradient of the NO_y /O_3 ratio measured on the ER-2 [*Fahey et al.,* 1985; *Proffitt and McLaughlin,* 1983], which is strongly negative toward the tropics and therefore can be used to identify tropical air [Murphy et al., 1993]. Typically, this resulted in the selection of data equatorward of 10° to 6°N.

The average extratropical mixing ratio profile for each species was synthesized in two steps. First, data taken by WAS and ALIAS between 30° and 55°N during STRAT and POLARIS were averaged into mean vmr profiles. We assumed that below the 420 K potential temperature surface, extratropical stratospheric profiles in each hemisphere are influenced by mixing with the upper troposphere. Above 420 K we assumed that the annual mean tracer distribution is identical for both hemispheres. This assumption is supported by satellite and aircraft observations of, for example, N_2O and CH_4 [Michelsen et al., 1998; Randel et al. 1993, 1998; Tuck et al., 1997a] that do not show clear evidence for a general interhemispheric asymmetry of tracer mixing ratios above the 420 K theta level. Also, recent 2-D and 3-D model calculations [X. X. Tie and W. Randel, private communication, 1999] do not point toward such an asymmetry. Please see section 5 for an examination of this topic using the Airborne Southern Hemisphere Ozone Experiment/Measurements for Assessing the Effects of Stratospheric Aircraft (ASHOE/MAESA) data set. Extratropical stratospheric profiles below 420 K were obtained by scaling the mean profiles measured in the Northern Hemisphere by half of the observed interhemispheric gradient of the mixing ratio of each species. The interhemispheric gradients (see Table 1) were calculated from data taken by the DC-8 WAS system [e.g., *Blake et al.,* 1996a] during the PEM-Tropics mission in early fall 1996 [*Hoell et al.,* 1999]. Only upper tropospheric measurements (i.e., from flight altitudes above 9 km) between 30°N and 55°N and between 30°S and 55°S were used. The vmr profiles derived in this manner were used to represent in the model the average composition of midlatitude air mixed into the tropics. The profiles are also plotted in Figure 5 for comparison with the tropical data.

Boundary conditions for the model were established using data obtained from the ER-2 during the tropical dives below 17.5 km altitude and from the DC-8 during PEM-Tropics at altitudes above 10 km within 5° of the equator. Tracer concentrations at the tropical tropopause were estimated from these observations (see Table 1) and used to initialize the model at the θ = 370 K level.

The 1-D model neglects vertical diffusion. *Mote et al.* [1998] and *Hall and Waugh* [1997] have shown that vertical diffusion has a small effect on the abundance of tropical tracers compared to the effect of vertical advection. Photochemical production and loss rates were computed for each species and potential temperature level using 24-hour average photolysis rates and concentrations of O^1D and Cl resulting from the average of full diurnal runs of the PSS model for tropical solar conditions of each season. Finally, the growth rate term in (1), $\gamma\chi$, was calculated from global mean tropospheric trends during the period 1994-1997 [*Alternative Fluorocarbons Environmental Suitability Study,* 1997; *Dlugokencky et al.,* 1997; *Fraser et al.,* 1998; *Montzka et al.,* 1996; *Travnicek et al.,* 1998; S. Montzka, private communication, 1999] (see Table 1). The growth rate was assumed to be negligible for CH_3Cl, CH_3Br, CO, ethane, and C_2Cl_4.

Lastly, seasonal variations in transport and photochemistry are not treated in the 1-D model. Limited tropical data (at most two flights per season) preclude us from performing a seasonally dependent analysis. With few tropical flights it is difficult to determine whether flight-to-flight differences in tracer concentrations represent seasonal variations in transport or merely the varying influence of different source regions on the tracer concentrations near the tropical tropopause. As a result of averaging 2 years of data, we also achieve better precision in the tracer profiles for each geographic region.

4. Results

Different transport processes and the chemical schemes applied in the model are examined in the following discussion. We note that all model runs shown in Figures 2, 3, and 4 and Plate 1 were performed using the optimized set of parameters, except for the parameter that was varied to demonstrate its influence on the model results. The process of finding the optimized set of parameters involved many iterations as well as extensive testing of different possible combinations of chemistry and transport that are not described for the purpose of clarity. However, the reader should bear in mind that we are using an independent estimate of the ascent rate based on radiative heating calculations (tested by comparison with tracer vmr profiles) and that the range of calculated concentrations of Cl is narrowed considerably by examining the in situ measurements of the short-

lived tracers. The discussion below is intended to demonstrate that the observed vmr profiles of individual tracers and the correlation of CO versus ethane do in fact provide a strong constraint on the mean ascent rate in the tropical upwelling region and on the mean chlorine atom concentration in the lower tropical stratosphere.

4.1. Short-Lived Species and Chlorine Chemistry

If τ_{chem} is small enough that the chemical loss term in (1) dominates the quasi-horizontal mixing term, the altitude profile of a tracer is primarily sensitive to chemistry and nearly independent of the entrainment time τ_e and the midlatitude vmr profile χ_{ML}. The simulation of measured tropical vmr profiles of CO, ethane, and C_2Cl_4, tracers with very short lower stratospheric lifetimes on the order of a few months, is discussed below and used to constrain the chlorine atom concentration and ascent rate profiles within the 1-D model. This provides greater confidence in the entrainment times derived from the 1-D model simulation of the vmr profiles of the long-lived species.

The Cl concentration is a critical parameter for the chemistry of the lower tropical stratosphere. It must be realistic to calculate accurate chemical loss rates of ethane, C_2Cl_4, and CH_4, as well as the production rate of CO. It is calculated in the standard version of the PSS model using total inorganic chlorine (Cl_y) as a direct input parameter, utilizing an empirical relationship between CFC-11 and Cl_y based on Airborne Chromatograph for Atmospheric Trace Species (ACATS) measurements of the major organic source molecules (CCl_y) [*Elkins et al.*, 1996]. Total inorganic chlorine is calculated from ACATS CCl_y using observed SF_6 concentrations to estimate the age of the sampled air mass in order to account for the slight decrease of CCl_y with time for the contemporary troposphere (J. Elkins, private communication, 1999).

The model probably tends to underestimate the actual Cl concentration in the lower tropical stratosphere when the ACATS relation for Cl_y is used. This Cl_y relation does not account for several short-lived organic chlorine-containing species that are not measured by ACATS, for example, methylene chloride, chloroform, and the bromochlorocarbons. This potential influence of short-lived source gases on lower stratospheric halogen chemistry has been suggested in the literature [*Ko et al.*, 1997; *Schauffler et al.*, 1999; *Solomon et al.*, 1994]. Many of these short-lived chlorinated species are measured by WAS and can account for more than 100 pptv of organic chlorine in the tropical upper troposphere. Also, several of the HCFC molecules with rapidly rising tropospheric concentrations are not included in the ACATS relationship. Furthermore, there are large uncertainties in the concentration of HCl in the lowermost tropical stratosphere. At the tropical tropopause, HCl mixing ratios calculated using the standard PSS model are 5 pptv or less. In contrast, during the POLARIS flight on 970923, the ALIAS observations of HCl at the tropical tropopause are close to the LOD but allow us to estimate an upper limit for the HCl mixing ratio of 200 pptv.

To investigate the model sensitivity to assumptions regarding Cl_y, we produced an alternative relation (referred to as the WAS/ALIAS relation) for Cl_y using total organic chlorine (CCl_y) as measured by WAS and HCl at the tropical tropopause measured by ALIAS. We calculated the mixing ratios of Cl_y on the basis of the average reduction of the WAS CCl_y at each potential temperature level compared to the average CCl_y at the tropical tropopause. A correction for the overall trend of the tropospheric total chlorine burden was not made for this calculation, but this is unimportant since the age of air in the lower tropical stratosphere is on the order of 1 year [e.g., *Boering et al.*, 1996]. Since the total chlorine burden of the troposphere is currently decreasing with time [*Hoffmann et al.*, 1998], not including a correction will give an upper limit with regard to Cl_y. The boundary condition for Cl_y at the tropical tropopause was set to 200 pptv, on the basis the upper limit for HCl observed by ALIAS. This estimate for Cl_y is based entirely on measurements and does not rely on any assumptions regarding unmeasured CCl_y species.

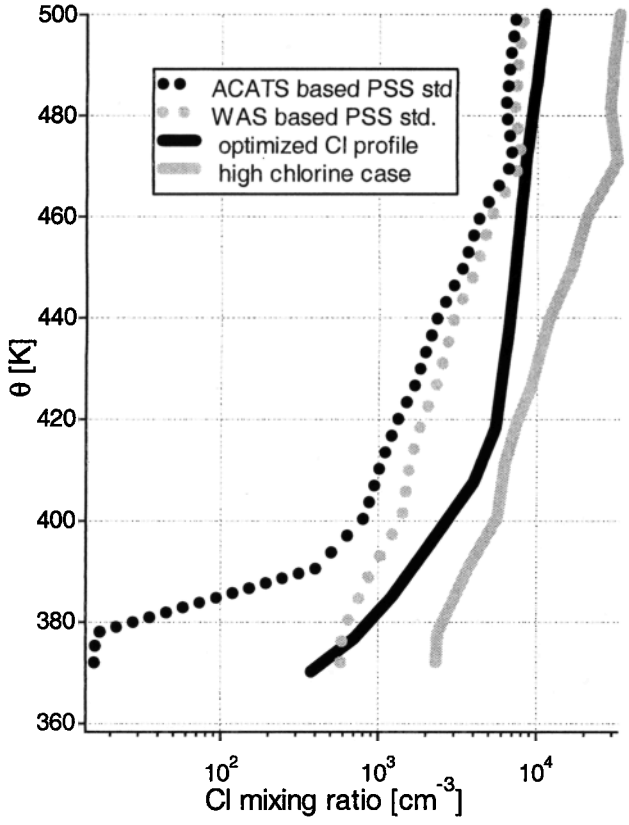

Figure 1. Chlorine atom concentration profiles versus potential temperature for the lower tropical troposphere. Compared are two photochemical steady state (PSS) model results for different input parameter sets, the upper limit chlorine atom concentration profile, and the optimum chlorine atom concentration profile retrieved to match the short-lived tracer observations. See text for details.

Figure 1 shows the chlorine atom concentration versus potential temperature calculated by the PSS model using both the ACATS and WAS/ALIAS assumptions for Cl_y. Also shown is the optimized chlorine concentration profile that provides best agreement with the measured mixing ratio profiles of ethane and C_2Cl_4 (see below). We also show a "high-Cl" profile in that was derived by multiplying the PSS model profile based on WAS/ALIAS Cl_y by a factor of 4. This high-Cl profile is used below to investigate the sensitivity of calculated profiles of CO, ethane, and C_2Cl_4 to assumptions regarding atomic Cl. The multiplicative factor of 4 used for this profile was arrived at on the basis of considering the uncertainties in Cl_y, uncertainties in the rate coefficients that describe the Cl/ClO ratio and the

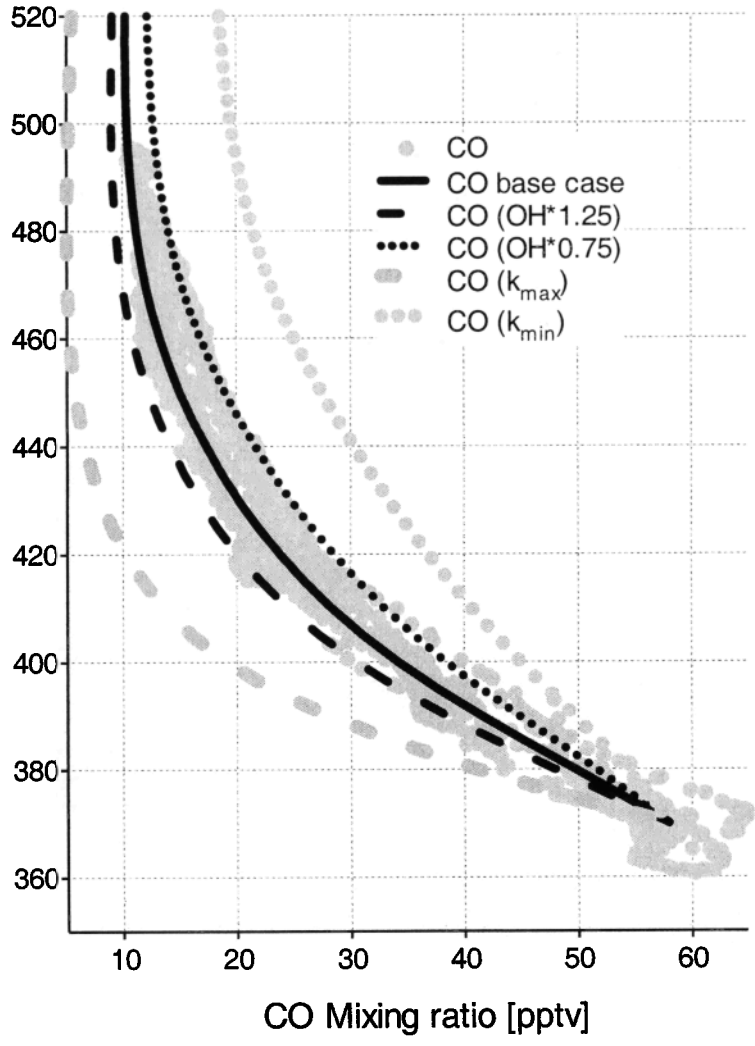

Figure 2. Measured and modeled tropical profiles of CO during STRAT/POLARIS. The dots represent the measurements by ALIAS, the black solid line is the CO concentration predicted by the 1-D model using measured OH radical mixing ratios. The black dotted and dashed lines are model runs using measured OH increased by 25% and reduced by 25%, respectively. The dotted and dashed gray lines represent the base case OH using the uncertainties of the rate coefficient for the reaction of CO with OH [*DeMore et al.*, 1997] (see text). All calculations are based on the average tropical ascent rates calculated by *Rosenlof* [1995].

reaction of OH + HCl near 200 K, as well as the tendency of the PSS model to underestimate the observed concentration of OH in the lowermost tropical stratosphere by nearly a factor of three (i.e., allowing in the PSS model for a "missing" source of HO_x strong enough to match measured OH will lead to a significant rise in calculated Cl due to the influence of the OH + HCl reaction). This multiplicative factor is unlikely to be realistic for the higher altitudes (e.g., $\theta > 460$ K) because theory and observation of OH are in much better agreement and the fractional uncertainty in Cl_y is much smaller. The large differences in the two PSS model profiles for Cl illustrated in Figure 1 demonstrate that our ability to estimate the concentration of atomic chlorine using the PSS model is rather limited for the tropical lowermost stratosphere. We therefore derived an optimized Cl concentration profile by running our 1-D model (e.g., equation (1)) to match the observed altitude profiles of the short-lived tracers. Ethane and C_2Cl_4 are particularly sensitive to the concentration of Cl in the lower stratosphere (their reaction rates with Cl are several hundred times faster than the rates for reaction with OH). Below ≈ 480 K, CO is relatively insensitive to Cl, but production of CO from CH_4 + Cl becomes important at higher altitudes.

Varying OH within the estimated measurement uncertainty has little effect on the model ethane and C_2Cl_4 profiles (e.g., <3% difference) and thus has little effect on the optimized concentration of Cl. It does, however, have a significant impact on the calculated profile of CO. Figure 2 shows the ALIAS CO data collected in the tropics and 1-D model results using the measured concentrations of OH (as presented by *Herman et al.* [1999]) and, for comparison, the calculated profiles of CO taking into account the measurement uncertainty of OH given by the Harvard group and the uncertainty of the rate coefficient for the reaction of CO with OH given by *DeMore et al.* [1997]. The measured vmr profile of CO, is in excellent agreement with

modeled CO using three independently determined parameters, that is, the measured concentration of OH, the recommended rate coefficient for OH + CO, and the mean tropical ascent rates calculated by *Rosenlof* [1995] (see section 3.3). This demonstrates that these parameters are reasonable and self-consistent [see also *Herman et al.*, 1999]. We did not vary the O^1D profile calculated using the PSS model because the impact of uncertainties in O^1D on the chemical loss rates of the species we analyze here is relatively small for the lower stratosphere (see Table 1). The photolysis rates calculated by the PSS model were also adapted into the 1-D model unchanged.

The optimized concentration of Cl lies within the range of the PSS model calculations, given the uncertainties in model input parameters described above. While it may be tempting to attribute the difference between the Cl profile found using the WAS/ALIAS constraint for Cl_y and to attribute the optimized Cl profile to the influence of heterogeneous processes not represented in the PSS model, we note that the calculated profile for NO agrees with observation to better than 20% between 380 and 420 K for the tropical flight of 970923. The tropical observations of NO obtained during STRAT and POLARIS suggest the heterogeneous sink of NO_x is treated in a reasonable fashion by the PSS model, although this conclusion is complicated by the inability of the model to properly simulate observed concentrations of OH [*Herman et al.*, 1999]. The large uncertainties in the rate coefficient for gas phase processes such as OH + HCl [e.g., *Michelsen et al.*, 1996, Figure 2], ClO + O, and Cl + O_3 for temperatures near 200 K as well as the uncertainty in the model profile for Cl_y make it unclear whether "missing chemistry" (such as heterogeneous reactions on cirrus clouds, as recently discussed in the literature [*Borrmann et al.*, 1996; *Solomon et al.*, 1997]) is necessary to explain the optimized profile for Cl derived from the tracer observations.

Figures 3a-3c show the measured mixing ratios of CO, C_2Cl_4, and ethane versus potential temperature, and Figure 3d shows a correlation plot of the measured mixing ratios of ethane versus CO. Also shown are 1-D model simulations using three profiles of 24-hour mean chlorine atom concentrations: (1) the PSS model Cl profile using the "standard" WAS/ALIAS Cl_y constraint, (2) the optimized Cl profile, and (3) the upper limit Cl profile (Figure 1). An entrainment time of 8.5 months was used in all cases (the entrainment time does not have a significant influence on the predicted altitude profiles of these species owing to their short photochemical lifetimes).

It can be seen in figure 3a that the upper limit chlorine profile is unreasonable since it significantly increases the steady state CO mixing ratio above 460 K, owing to increased production from the reaction of chlorine atoms with CH_4. At potential temperature levels below 440 K the chlorine atom concentration does not significantly change the calculated CO mixing ratio but has a strong influence on the calculated profiles of ethane and C_2Cl_4, as demonstrated in Figures 3b and 3c. Although the optimized Cl profile somewhat underestimates the observed vmr of CO and ethane around 440 K, it fits the observed CO to ethane ratio very well, as shown in Figure 3d. At 440 K, model CO and ethane are in good agreement with the measurements taken during the flights of 951105, 960213, and 961211. The measurements from flights 960801 and 970923 are underestimated by the model, probably because it does not treat seasonal variations. In fact, much of the scatter in tropical stratospheric CO may be due to seasonal variations in the vmr of CO of air entering the stratosphere at the tropical tropopause, but a close examination of those variations would be beyond the scope of this paper (see also section 4.4) [*E.J. Moyer*, private communication].

The optimized chlorine profile also fits the observed altitude profile of C_2Cl_4, given that the data exhibit significant scatter. This scatter is probably attributable to the large interhemispheric gradient of C_2Cl_4 in the upper troposphere as well as to background levels in some sample flasks (see below). We note, however, that the kinetic data recommended for the reaction of C_2Cl_4 with OH by *DeMore et al.* [1997] did not allow for a reasonable fit of the C_2Cl_4 altitude profile. A new measurement of this rate constant made by R. Talukdar, (private communication, 1999), who reports the same room temperature rate coefficient but a significantly smaller temperature dependency for this reaction than given by *DeMore et al.* [1997], leads to a much faster rate coefficient under lower stratospheric conditions (e.g., a factor of 4 increase at 200 K). Our model results are based on these new laboratory data.

Both C_2Cl_4 and ethane show measurable mixing ratios above the 460 and 470 K levels, respectively, even though the modeled mixing ratios approach zero. This is likely caused by a small measurement artifact related to outgassing of the canister walls, the inlet line, and/or the inner surfaces of the pump. These background levels vary between 0 and 20 pptv of ethane and between 0 and 0.1 pptv of C_2Cl_4, which makes it very difficult to correct each individual canister but may, on the average, account for the "residual" concentrations measured at high altitudes. Removing an average artifact of 15 pptv for ethane and 0.05 pptv for C_2Cl_4 produces negative concentrations for about 30% of the samples but overall improves the model/measurement comparison at the highest altitudes.

In summary, we believe that the chlorine atom concentration profile inferred from the short-lived tracer measurements provides a better estimate of the actual concentration of Cl than the concentration of Cl calculated by the PSS model owing to uncertainties in Cl_y and relevant kinetic processes. Without changing any other chemical loss variables, the optimized profile of Cl provides a very good fit to the observed altitude profiles of different species that have very different sensitivities to the concentration of Cl.

4.2. Ascent Rates

The stated uncertainty of the ascent rates used in the 1-D model is on the order of ±50%, on the basis of the inherent uncertainties of heating rate calculations [*Rosenlof*, 1995]. This raises the question of whether it may be possible to find a different combination of entrainment rates and chemical conditions that would offset a change in the model ascent rate profile and still fit the observed tracer profiles. Figure 4a demonstrates that the observed vmr profile of CFC-12 can be adequately simulated by using a 30% reduction of the ascent rates and an entrainment time of 13.5 months [*Volk et al.*, 1996] instead of our optimized entrainment time of 8.5 months (see below). Similarly, the observed CFC-12 profile can be simulated reasonably well using the entrainment times calculated by *Mote et al.* [1998] or *Minschwaner et al.* [1996], or even allowing for unmixed ascent, provided the ascent rates are further reduced. Figure 4b demonstrates that the observed ethane profile can be simulated adequately only if the 30% slower ascent rates are combined with a much lower chlorine atom concentration because ethane is sensitive to ascent rate and Cl concentration but not to entrainment time. The observations of CO are simulated well using the standard ascent rate profile (Figure 2),

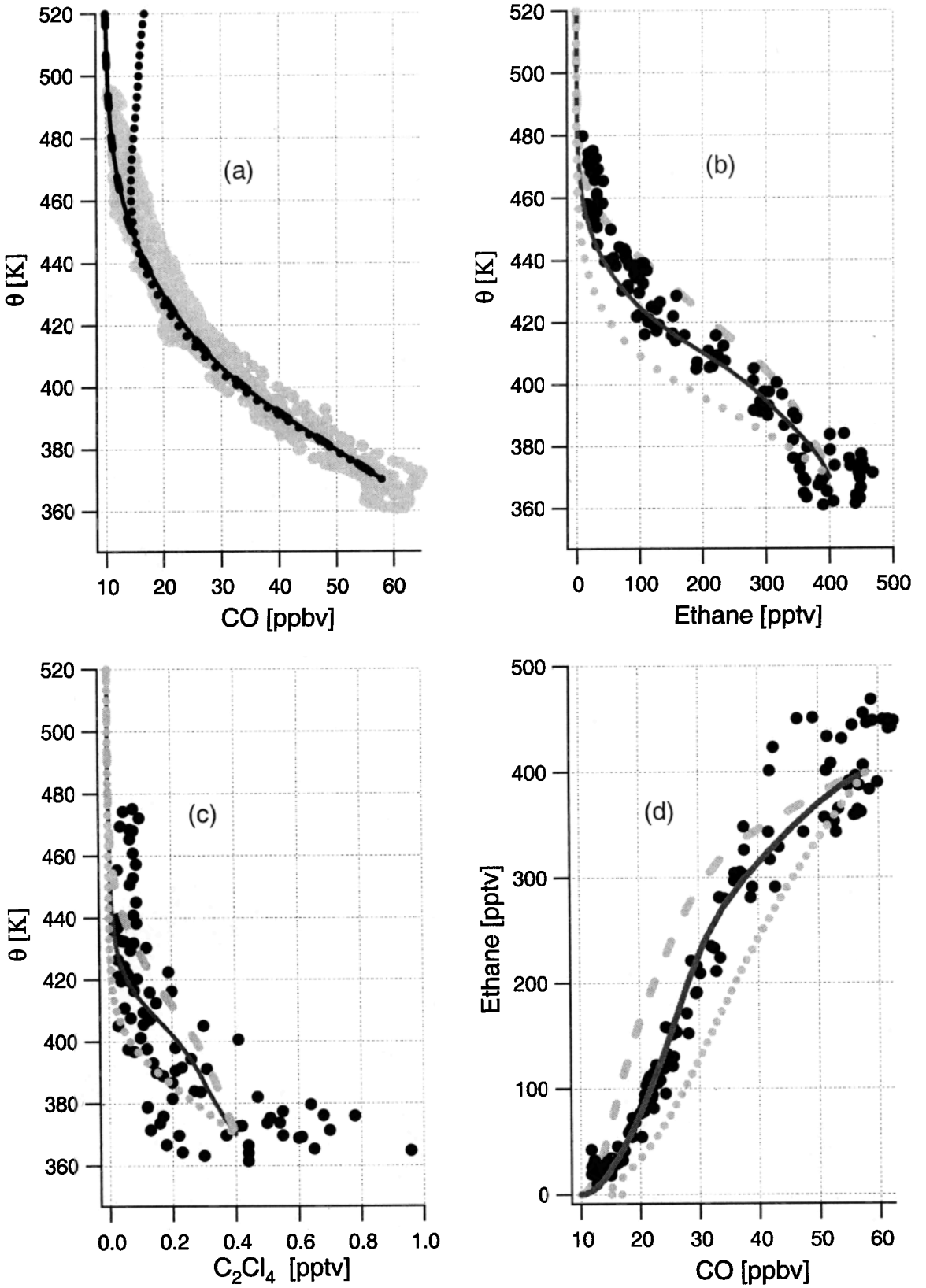

Figure 3. Mixing ratios of (a) CO, (b) ethane, and (c) tetrachloroethene in the tropical lower stratosphere versus potential temperature. Plotted are the individual measurements (solid circles) and 1-D model results using three different chlorine radical altitude profiles. Profiles were calculated by the PSS model using the standard input data set based on the WAS measurements (dashed line) and the upper limit chlorine concentration from the PSS model (dotted line). The solid line is the tracer profile calculated by the PSS model using the optimum chlorine atom concentration to achieve a good fit with the measurements. Figure 3d is a correlation plot of CO versus ethane. The model results are shown as in Figures 3a-3c. The higher-resolution ALIAS data (3-s) was averaged over the WAS can sampling intervals to allow direct comparison.

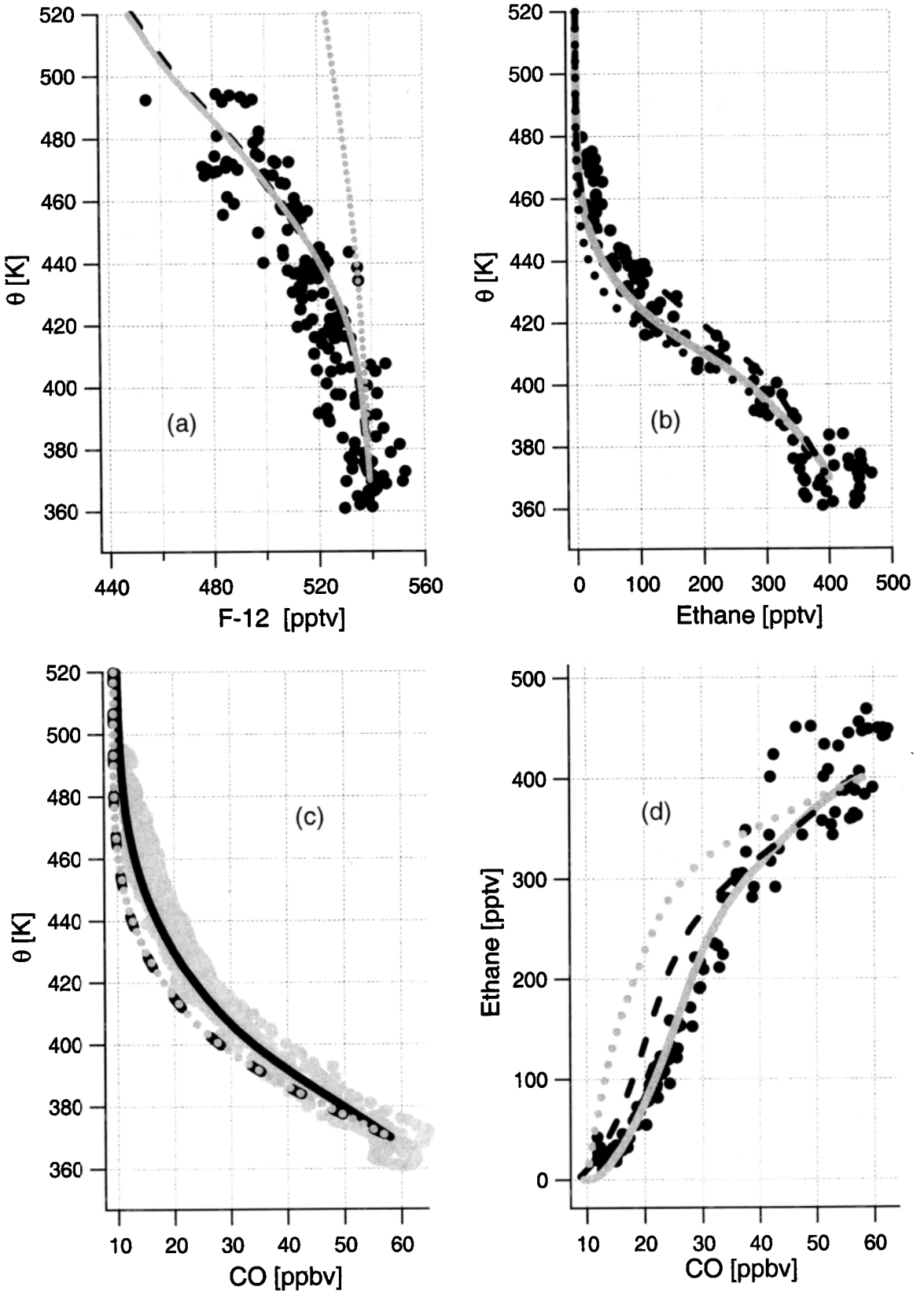

Figure 4. (a) CFC-12 mixing ratios (solid circles) versus potential temperature in the tropics. Shown are 1-D model results for the 8.5-month entrainment time with unaltered ascent rates (reference case: solid line) and for a 13.5-month entrainment time [*Volk et al.*, 1996] using ascent rates that were 30% slowed (dashed line). Also shown is a result for the tropical pipe model with 30% slower ascent rates for comparison (dotted line). (b) Ethane and (c) CO mixing ratios in the tropics versus potential temperature (filled circles). Also plotted are the reference case (solid line) and the 1-D model results for 30% slowed ascent rates and 13.5-month entrainment time with unaltered chemistry (dashed line) and lower chlorine atom concentrations (dotted line). (d) As in Figures 3b and 3c, but for the CO/ethane correlation.

but there may be other combinations of ascent rates, OH concentrations, and rate coefficients for OH + CO within their respective error bars (see also section 4.1) that would also provide a good fit to the measured tracer profiles For instance, CO is simulated well with 20% lower OH concentration and 10% slower ascent. The calculated profile of CO is sensitive primarily to ascent rate and the rate of removal by reaction with OH but insensitive to moderate changes in chlorine as well as entrainment time (see Figure 4c). The accuracy of the standard ascent rate profile is further demonstrated in Figure 4d, which shows the 1-D model estimate for the CO/ethane correlation for various scenarios.

The uncertainty of the rate coefficient for OH + CO given by *DeMore et al* [1997] is +90%, -50% for lower stratospheric temperatures and pressures, largely owing to the published uncertainty of the temperature-dependent term (e.g., *E/R*). The uncertainty factor for *E/R* given by *DeMore et al.* [1997] is for 1 atmosphere of air. The laboratory study of *Hynes et al.* [1986] concludes the uncertainty of this term is considerably smaller, over a range of pressures from 70 to 1000 mbar, than the value given by *DeMore et al.* [1997]. We have adopted a ±30% overall uncertainty of the rate coefficient for OH + CO, which brackets the laboratory data from several groups summarized by *Hynes et al.* [1986, Table 2]. This is more representative of the true uncertainty in the rate of this reaction for stratospheric conditions (W. B. DeMore, private communication, 1999) than the *DeMore et al.* [1997] value, which applies to tropospheric conditions. Our calculations suggest the ascent rates are accurate to ±44% if one assumes a 30% uncertainty in measured OH, 30% uncertainty in the OH + CO rate coefficient, and 10% uncertainty due to CO variations.

4.3. Long-Lived Species

If the chemical loss term in (1) is small compared to the quasi-horizontal mixing term, the simulated altitude profiles should be mostly sensitive to the entrainment times and the entrained midlatitude mixing ratios. The relative influence of chemistry should increase with decreasing lifetime. Plates 1a-1i show the measured vmr profiles in the tropics for CH_4, CFC-11, CFC-12, CFC-113, CFC-114, CH_3Cl, CH_3Br, H-1211, and H-2402, respectively Also plotted are the average midlatitude profiles used as input for the 1-D model (see section 3) and results from our 1-D model simulations. Profiles were computed using the tropical pipe model (with chemical losses only, i.e., no entrainment of midlatitude air) and for five other entrainment time schemes: altitude independent averages for τ_e of 4 months, 8.5 months, and 13.5 months (as calculated by *Volk et al.* [1996]) and two different altitude-dependent entrainment time profiles as calculated by *Mote et al.* [1998] and *Minschwaner et al.* [1996]. Both of these latter studies have relatively slow entrainment over the 16- to 20-km altitude range, slightly slower than the 13.5-month average based on the study by *Volk et al.* [1996] (see section 5 for further discussion of these studies compared to our result). For clarity, not all model results are shown for all species in Plate 1.

The tropical pipe model has chemistry as the sole loss term, and thus finds very small vertical gradients for the longest-lived tracers such as CH_4, CFC-12 and CFC-114. The data clearly show that the observed concentrations are significantly overestimated when unmixed ascent is assumed. Because the altitude profiles of all long-lived species, as expected, exhibit lower vmrs in photochemically older air at midlatitudes, stronger mixing (i.e., shorter entrainment times) into the tropical upwelling region causes the concentrations in the tropics to fall off more quickly with altitude. Consequently, the different entrainment time schemes predict stronger altitude gradients as the characteristic entrainment time decreases. The calculations based on the *Mote et al.* [1998] and *Minschwaner et al.* [1996] entrainment rates result in considerably smaller altitude gradients than observed.

The best fit to all of the measured species is achieved using an altitude-independent entrainment time of 8.5 months. Simulations using a 4-month entrainment time are shown to demonstrate the sensitivity of the calculated profiles to a 50% reduction in the entrainment timescale. The simulation using $\tau_e = 4$ months clearly underestimates the observed vmr profiles of all species. We would like to emphasize that the entrainment time of 8.5 months provides an excellent overall fit to a set of compounds spanning a range of photochemical lifetimes of 1.5-350 years at 420 K. The simulations for various τ_e of species that are more strongly influenced by local chemistry (e.g., methyl bromide and the halons) are less separated, as expected, than the simulations for various τ_e of the longer-lived species. However, the 8.5-month entrainment time still can be identified as the best representation of the shorter-lived species because the altitude profiles are more pronounced and the data exhibit less scatter (with the exception of H-2402, which has very low concentrations close to the LOD). Our conclusions are further supported by excellent agreement between model and measurements of tracers that have different chemical loss mechanisms and altitude dependencies of their loss rates, for example, CH_3Cl (whose lifetime decreases by only a factor of 2 between 370 and 500 K) and CFC-11 (whose lifetime decreases by a factor of 15 between 370 and 500 K; see Table 1).

It is conceivable that there is vertical structure to the entrainment times for potential temperature levels below 520 K, for example, faster entrainment at lower altitudes. However, the scatter in the data, especially the lower altitude observations, does not allow us to extract information concerning the altitude dependence of τ_e. For example, if we assume an increasing value of τ_e with altitude (e.g., slower entrainment with increasing altitude) by scaling the shape of the entrainment time profile of *Mote et al.* [1998] to an average of 8.5 months between 16 and 20.5 km, the calculated tracer profiles are similar to those shown in Plate 1 for $\tau_e = 8.5$ months and provide an equally good fit to the observed profiles. The observations would have to be exceedingly accurate, precise, and representative of mean tropical conditions in order to identify an altitude dependent shape of τ_e.

4.4. Uncertainty

It is very difficult to mathematically describe the overall uncertainty of our model results for τ_e. Uncertainties are introduced by variations in the input data, error bars on the kinetic data, and empirical relationships applied in the PSS model. As discussed above in section 4.2, the uncertainty of some of these input parameters (e.g., chlorine radical concentrations and ascent rates) can be better constrained by our simulations of specific species compared to their "allowable" uncertainty from independent estimates.

The scatter in our measurements of both tropical and midlatitude tracer profiles introduces additional uncertainty into the estimate of τ_e. This scatter is caused in part by limitations of the instrumentation in the case of the longest-lived species since the observed decrease of the mixing ratios of the CFCs, CH_4, and CH_3Cl is on the order of only 5-10% over the entire altitude

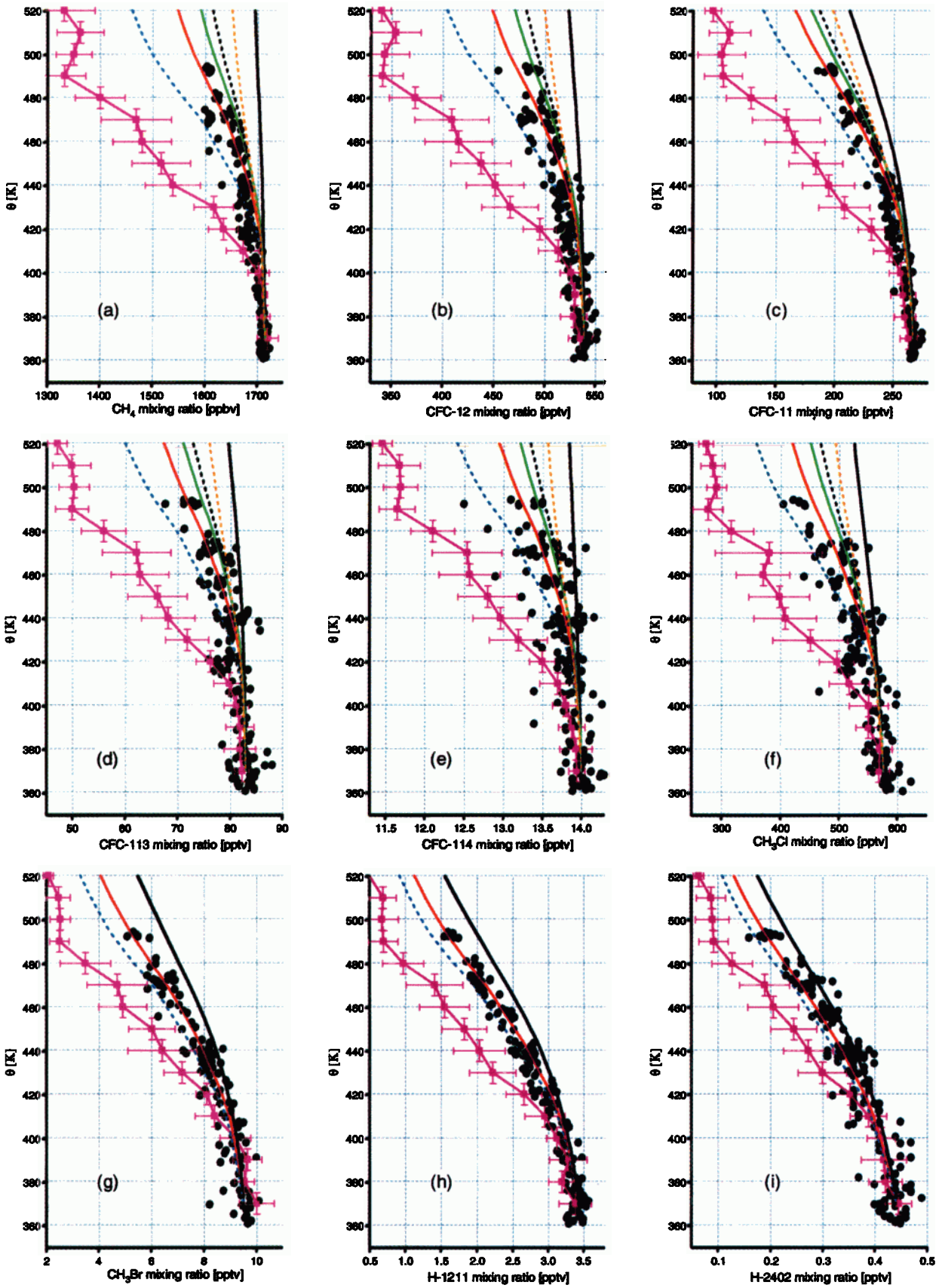
θ [K]
(a)
CH4 mixing ratio [ppbv]
(b)
CFC-12 mixing ratio [pptv]
(c)
CFC-11 mixing ratio [pptv]
(d)
CFC-113 mixing ratio [pptv]
(e)
CFC-114 mixing ratio [pptv]
(f)
CH3Cl mixing ratio [pptv]
(g)
CH3Br mixing ratio [pptv]
(h)
H-1211 mixing ratio [pptv]
(i)
H-2402 mixing ratio [pptv]

range. This is a small change, only about a factor of 5 or so larger than the overall precision of the measurement. Additional scatter may be produced by weak seasonal variations in the tropospheric concentrations (e g., in the case of CH_4, CO, and CH_3Cl). Another factor is the area in which the flights were performed. The typical seasonal variation in the synoptic conditions in the Pacific south of Hawaii changes the source areas from which air is brought to the region [e.g., *Hess et al.*, 1996]. Both CH_4 and methyl chloride have significant biomass-burning sources [*Blake et al.*, 1996b], methyl chloride also has a marine source, and CFCs are mainly emitted from urban areas. The combination of these effects can cause variations in the boundary conditions (reflected in the scatter at the lowest altitude level) that propagate to higher altitudes in the tropics. However, these factors will cause systematic errors in our estimate of τ_e only if any of the different source regions would be more strongly represented during certain sampling times than others. Since the study was carried out over a time of almost 2 years and since the photochemical ages of the air masses sampled at higher altitudes in the tropics span another 2 years or so, none of these effects should cause errors that are larger than those represented by the scatter of the observed data.

Since the most sensitive input parameter is the midlatitude profile, we performed simulations for selected tracers using the upper and lower standard deviation of the midlatitude profiles as model input. The average values of τ_e resulting from simulations of CH_4, CFC-11, CFC-12, and CFC-113 are 13.0 months for the upper limit of the midlatitude profiles and 5.5 months for the lower limit. These limits would also encompass more than 90% of the single measurements of all tracers made above 440 K in the tropics. We therefore report an average characteristic entrainment timescale of 8.5^{+6}_{-4} months.

This range for the entrainment timescale also encompasses the values for τ_e found using the various (individual) assumptions regarding the concentration of atomic Cl described above, the ±44% uncertainty for the ascent rate estimated on the basis of the comparison of modeled and measured CO, and the ±25% uncertainty in measured OH. While the uncertainties in most of the rate coefficients of the key loss terms are also encompassed by the 8.5^{+6}_{-4} month range for τ_e, we note that consideration of the *DeMore et al.* [1997] uncertainties for the kinetic processes that limit production and loss of CO would lead to a larger range for τ_e. However, as suggested earlier by *Herman et al.* [1999], we show in Figure 2 that the actual combined uncertainties of the rate coefficients for the CO production and loss reactions are considerably smaller than the combined uncertainties given by *DeMore et al.* [1997].

5. Discussion

The sensitivity analysis described above provides reasonable evidence that the uncertainty in the model parameters for ascent rates and the concentration of Cl yields a well-constrained mean entrainment timescale of 8.5^{+6}_{-4} months averaged over the altitude range of 16-20.5 km. We have shown that the model ascent rates cannot be slowed down or increased by more than 44%, because attempts to offset this by changing the chemistry and/or the entrainment timescale give model results that do not agree with at least some of the measured tracer vmr profiles Similarly, a change of the entrainment timescale cannot be offset with slowed or accelerated chemistry without failing to simulate one or more of the observed tracer profiles, which provides a high level of confidence in the accuracy of our retrieved parameters.

Our value for the average entrainment timescale of 8.5^{+6}_{-4} months agrees well with results from two recently published studies. *Herman et al.* [1999] used the same basic model approach to simulate altitude profiles of N_2O and CH_4 measured between the surface and 32-km altitude by the ALIAS II balloon-borne instrument. They calculated a value for τ_e of 6 months for altitudes below 20 km and of 16 months between 20- and 28-km altitude. An estimate for τ_e of about 5.5-7 months can be inferred from observations published by *Tuck et al.* [1997a] (see Figure 18 in that review). This result is not based on chemical tracer observations but uses a statistical analysis of 880 individual European Centre for Medium-Range Weather Forecasts (ECMWF) back trajectories to infer the percentage of air within 10° of the equator originating from midlatitudes as a function of potential temperature.

However, our result for τ_e is significantly different from the entrainment times calculated by *Volk et al.* [1996], *Minschwaner et al.* [1996], and *Mote et al.* [1998]. Use of their values for τ_e in our model, as shown in Plate 1, leads to similar altitude profiles of the long- and medium-long-lived tracers that exhibit a smaller vertical gradient than the observed profiles. Whether these discrepancies can be explained by different models, measurements, or methods used to derive the entrainment times is discussed below.

The study by *Mote et al.* [1998] is based on harmonic analysis of water vapor and CH_4 observations made by the Halogen Occultation Experiment (HALOE) instrument. The calculated entrainment time is less than 5 months at 16 km and then increases sharply to more than 30 months at 20-km altitude. However, especially below 19 km, where our results are very well constrained by the short-lived tracers, the HALOE data are quite uncertain and the results of *Mote et al.* [1998] are largely

Plate 1. Long-lived tracer mixing ratios as measured in the tropical lower stratosphere versus potential temperature θ. Plotted are the individual samples (black dots) and the 1-D model results for tropical pipe (black solid line), entrainment times as calculated by *Mote et al.* [1998] (orange dotted line), *Minschwaner et al.* [1996] (gray dashed line), and *Volk et al.* [1996] (green solid line), and entrainment times of 8.5 months (red solid line) and 4 months (blue dashed line). Also shown are the measured midlatitude profiles of the respective tracer (magenta solid line). The data are averages over 5° potential temperature intervals, the vertical error bars show the ranges of θ, and the horizontal error bars are 1σ standard deviations of the measurements. Tracers shown are (a) CH_4, (b) CFC-12, (c) CFC-11, (d) CFC-113, (e) CFC-114, (f) CH_3Cl, (g) CH_3Br, (h) H-1211, and (i) H-2402. Note that not all model results are shown for all species.

based on extrapolation. In the middle stratosphere, where HALOE provides very accurate measurements, the entrainment times calculated by *Mote et al.* [1998] are somewhat larger than those calculated by *Herman et al.* [1999] but have overlapping error bars.

Minschwaner et al. [1996] also calculated a slower entrainment timescale than found here, increasing from 4 to about 18 months for the 16- to 20-km altitude range, respectively, on the basis of an analysis of balloon and aircraft in situ measurements of N_2O [*Goldan et al.*, 1980, 1981; *Vedder et al.*, 1981, 1978]. Minschwaner et al. also calculate entrainment rates on the basis of N_2O data collected on the ER-2 during ASHOE/MAESA and Stratospheric Photochemistry Aerosol and Dynamics Experiment (SPADE) (lower stratosphere) and from the Cryogenic Limb Array Etalon Spectrometer (CLAES) instrument on board the UARS satellite (middle stratosphere) which yield faster mixing (τ_e increasing from 7 to 14 months between 380 to 470 K, respectively). However, the Goldan-Vedder N_2O data agree better with the ALIAS II based results for the middle stratosphere. Additional estimates of τ_e are made on the basis of observations of CFC-11. The large scatter, especially in the Goldan-Vedder and CLAES N_2O observations and the large differences between the individual estimates of τ_e based on the various data sets, results in an overall uncertainty of more than 50% below 500 K in the entrainment time estimates by *Minschwaner et al.* [1996], increasing to nearly 100% at lower altitudes.

In contrast, the study by *Volk et al.* [1996] is entirely based on data obtained with the ER-2 at altitudes between 16 and 21 km. A suite of compounds are used with comparably long atmospheric lifetimes to these considered in our study, with H-1211 being the shortest-lived species analyzed. Individual entrainment times were inferred from the correlations of each tracer with either ozone (NO_y, CFC-113, CFC-12, N_2O, and CH_4) or N_2O (H-1211, methyl chloroform, CCl_4, and CFC-11), which were then averaged to give a value for τ_e of 13.5 months. Although the individual error bars applied to most of the species at the low end of the photochemical lifetimes covered overlap with our result, the uncertainties attributed to entrainment times inferred from the longer-lived species did not. The photochemistry used by Volk et al. is based on the same PSS model used here. There are only a few slight differences between the lifetimes reported by Volk et al. and our calculation (see Table 1) that can be explained by differences in the radical field calculated by the PSS model or by different growth rates prior to 1994 compared to 1996-1997. However, there are significant differences between the tracer profiles that were measured at midlatitudes reported by Volk et al. and the midlatitude tracer profiles used here. This is demonstrated in Figure 5, using CFC-113 as an example. To investigate this further, we simulated the ASHOE/MAESA 1994 data that was used by Volk et al. with our 1-D model. Our results do agree very well with those of Volk et al., producing best fit entrainment times of 17 months for N_2O and CFC-12 and 32 months for CFC-113 [see *Volk et al.*, Figure 4 [1996,].There are several possible explanations for the apparent change in τ_e between 1994 and the time period of our study (1995-1997), which are discussed below.

First, the lower stratospheric dynamics during ASHOE/MAESA may have indeed been different than during STRAT/POLARIS. While our study covers a time period of about 2 years, and therefore averages over a complete period of

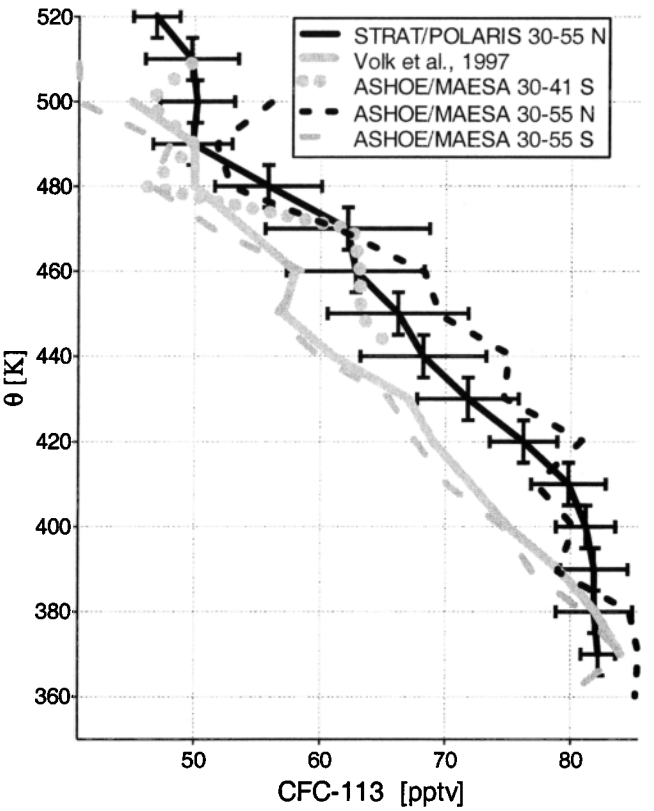

Figure 5. Comparison of the midlatitude CFC-113 volume mixing ratio (vmr) profile versus potential temperature θ as measured by *Volk et al.* [1996] (gray solid line, no standard deviations available) and in this study (black solid line). Error bars are θ range in the vertical and 1σ standard deviations in the horizontal. The dashed gray and black lines show the averaged midlatitude vmr profile of CFC-113 measured by ACATS during ASHOE/MAESA between 30° and 55°S and between 30° and 55°N, respectively. The gray dotted line depicts the average CFC-113 vmr profile measured during ASHOE/MAESA for the 30°-41°S latitude band (see text).

the QBO, ASHOE/MAESA was carried out between March and November 1994 [*Tuck et al.*, 1997b]. This period marks the end of an easterly phase of the QBO, which may have had an influence on the tracer altitude profiles owing to increased downward transport at midlatitudes. This enhanced downwelling may reduce the mixing ratio of CH_4 by up to 10% between 30°S and 45°S and between the 100 and 65 mbar pressure levels compared to the 2-year average mixing ratios (W. Randel, private communication, 1999). Similar reductions in the mixing ratios of the other long-lived tracers may be conceivable, potentially inducing a low bias to the data used by *Volk et al.* [1996] compared to the long-term mean profile at midlatitudes. The impact of the QBO on transport between the tropics and midlatitudes is not clear. Numerous tracer observations have shown that the subtropical gradient becomes stronger or weaker depending on the phase of the QBO (e.g., *Trepte and Hitchman*, 1992). However, *Polvani et al.* [1995] argue that a stronger subtropical gradient does not necessarily imply slower transport out of the tropics, and *Waugh* [1996] concludes that transport out of the tropics is insensitive to the phase of the QBO. Also, the amplitude of the QBO decreases with altitude in the

stratosphere [*Andrews et al.*, 1987]. Our data set also did not show significant differences in the midlatitude profiles of long-lived tracers between the two phases of the QBO that were covered.

The different tracer distributions observed in 1994 could also reflect interannual variations in stratospheric dynamical activity independent of the QBO. A second possible explanation arises from perturbations in heating due to enhancements in stratospheric aerosol loading immediately following the eruption of Mount Pinatubo in June 1991. These perturbations had a large effect on the stratospheric circulation [e.g., *Grant et al.*, 1992; *Kinne et al.*, 1992]. It has recently been suggested that HALOE observations of a ~15% reduction in the mixing ratio of upper stratospheric CH_4 between 1991 and 1997 was due to a longer-term effect of Pinatubo aerosols on stratospheric circulation [*Nedoluha et al.*, 1998]. If this hypothesis is shown to be correct, then it is possible that residual effects of the Pinatubo aerosol may be responsible for the significant differences in the midlatitude tracer profiles observed between 1994 and 1996-1997. However, one would expect such differences to be important only in the middle and upper stratosphere. In 1994, midlatitude lower stratospheric air parcels would be too young to be significantly affected by the Pinatubo aerosol from 2 years earlier. Figure 5 shows that the differences in midlatitude tracer profiles extend downward below 400 K, suggesting that Pinatubo aerosol are unlikely to be the cause.

A third possible explanation arises from the fact that the *Volk et al.* [1996] midlatitude profiles are mostly from data acquired in the Southern Hemisphere (SH), while our midlatitude profiles are comprised exclusively of Northern Hemispheric (NH) observations. Since there is stronger planetary wave activity in the NH than in the SH, a possible result could be a real asymmetry in the mixing processes of the lower stratosphere caused by more vigorous mixing between the tropics and midlatitudes in the NH compared to the SH. Since SH data is not available from STRAT/POLARIS but some NH data was taken during ASHOE/MAESA, we have tried to find evidence for such an asymmetry in the ASHOE/MAESA data set. Figure 5 shows that the average vmr profile of CFC-113 at northern midlatitudes exhibits considerably larger mixing ratios that are similar to or even slightly exceed the average midlatitude calculated from STRAT/POLARIS. Similar results are obtained for other tracers, such as CFC-12, CFC-11, N_2O, and CH_4. Also shown is the Southern Hemisphere midlatitude (30°-55°S) profile for CFC-113 during ASHOE/MAESA, which shows slightly lower CFC-113 values than those used by Volk et al., which is to be expected since SH data constitute about 90% of the observations used by Volk et al.

While similar latitude bands (30°-55°N in this study, 35°-55°N and S in *Volk et al.* [1996]) were used in both studies to define the midlatitude profiles, the spatial coverage of the two study areas are quite different and may also bias the retrieved midlatitude tracer profiles. The dominant fraction of the midlatitude data used by *Volk et al.* [1996] was acquired in the Southern Hemisphere during flight operations out of Christchurch, New Zealand, situated at 44°S and 167°E, between April and October 1994, whereas most of the NH data was obtained during ascent and descent data taken from flights out of ARC (37.4°N, 122.0°W) in February-March and November 1994. The STRAT/POLARIS midlatitude profiles were also mainly synthesized from "stair-step" flights based out of ARC with a contribution from the northern sections of transit flights between ARC and Hawaii that included a dive between 30° and 33°N. A few points exhibiting a tropical signature (as determined by the NO_y/O_3 ratio) were filtered out of our midlatitude data set.

Therefore, as a fourth possible explanation, the difference in the vmr profiles could also be caused by a latitudinal gradient in tracer concentrations rather than or in addition to a possible interhemispheric difference. An attempt to investigate this further is shown by the dotted gray line in Figure 5. We have constructed an average SH vmr profile of CFC-113 from the ASHOE/MAESA data set that is more representative of the average latitude (37°N) of the STRAT/POLARIS data. To arrive close to this average latitude value for the ASHOE/MAESA observations from the SH one must eliminate of the data south of 41°S. Consequently, Figure 5 shows a vmr profile constructed from all measurements obtained between 30° and 41°S. Except for the 480-K level, this profile shows considerably larger vmrs of CFC-113 than the profile used by *Volk et al.* [1996] and, within the error bars, agrees with the STRAT/POLARIS midlatitude profile used in our study. Unfortunately, since all lower altitude data from the ASHOE/MAESA SH midlatitude flights are ascents or descents over Christchurch, no data is available below the 440 K level. However, assuming the trend toward larger concentrations continues for lower altitudes, a latitudinal gradient of tracer concentrations would explain most of the discrepancy between the STRAT/POLARIS vmr profiles and the ASHOE/MAESA profiles used in the Volk et al. study.

This latitudinal gradient is consistent with the downward sloping and poleward sloping tracer isopleths expected from the stratospheric general circulation [e.g., *Andrews et al.*, 1987]. Another possible explanation for this latitudinal gradient of tracer profiles could again be the sampling location of the ASHOE/MAESA flights in the SH. Especially during the late phase of the experiment, the edge of the Antarctic vortex was observed as far north as 53°S. *Tuck et al.* [1997a] and *Rosenlof et al.* [1997] conclude that vortex edge air may have been mixed into the midlatitude lower stratosphere during the Antarctic spring deployment. It is therefore conceivable that the midlatitude profiles used by *Volk et al.* [1996] may include some air masses of polar character, thus biasing the average altitude profiles of the long-lived species to lower concentrations than what may be characteristic for air that typically mixes into the tropical upwelling region. This is particularly important since the data were filtered only by latitude (M. Volk, private communication, 1999).

While a latitudinal gradient of the midlatitude tracer profiles remains the most likely explanation for differences in τ_e found here compared to those reported by *Volk et al.* [1996], all of the effects described above may have had an influence on the calculated entrainment time. With the limited measurement data available to date, it is not possible to clearly distinguish between various effects.

6. Conclusions and Atmospheric Implications

This study is the first analysis to investigate lower stratospheric dynamics in the tropics using a set of tracers with such a large span of photochemical lifetimes (less than 1 month to 350 years at 420 K). We have used measured vmr profiles of C_2Cl_4, ethane, and CO and the CO versus ethane correlation plot to constrain the parameter set used in our model to simulate the

observed altitude profiles of the longer-lived species. The measured tropical vmr profiles of all species examined here can be described with a single average entrainment timescale of 8.5^{+6}_{-4} months for the 16- to 20.5-km altitude band, one unique (annually averaged) profile of radical concentrations and photolysis rates, and a single mean ascent rate profile representative of the 2-year observational period. The calculated profile of CO is very sensitive to heating rate Q (on which the ascent rate is based [*Rosenlof,* 1995]) and the concentration of OH [*Wennberg et al.*, 1998]. Excellent agreement between the observed CO and the 1-D model indicates that we can have a high level of confidence in the radiative heating rates and the mean OH concentration derived from in situ measurements of OH. The observed profiles of C_2Cl_4 and ethane are used to optimize the concentration of Cl, which is quite uncertain owing to limited knowledge of Cl_y and key kinetic parameters in the cold lowermost stratosphere.

Our analysis yields an entrainment timescale that is shorter than that reported by earlier studies [*Minschwaner et al.*, 1996; *Mote et al.*, 1998; *Volk et al.*, 1996] but agrees well with two recently published estimates for τ_e [*Herman et al.*, 1998; *Tuck et al.*, 1997a]. We are able to reproduce the *Volk et al.* [1996] estimate of 13 months for τ_e using their observations and our model, demonstrating that this difference is not model dependent (the two models share many similar components). The discrepancy appears to be mainly attributable to a latitudinal gradient in tracer profiles and the fact that our midlatitude observations were obtained, on the average, closer to the tropics than the data used by Volk et al. However, we cannot completely rule out an interannual variability in the entrainment times that may be caused by the QBO, by residual effects of the Mount Pinatubo eruption in 1991, or by an asymmetry between the mixing from the two hemispheres into the tropics. Furthermore, the midlatitude observations used by *Volk et al.* [1996] may have been influenced by air from the Antarctic polar vortex. The differences between the value of τ_e found here and those reported by *Minschwaner et al.* [1996] and *Mote et al.* [1996] may be caused mainly by inaccuracies in the satellite observations in the lower stratosphere used in these studies and are reflected in their stated uncertainties for this region.

A shorter entrainment timescale allows for extratropical air to more quickly mix into the large-scale tropical ascent region than previously believed. This has a direct impact on assessment models used, for example, to simulate the influence of aircraft emissions (particularly those of a potential high speed civil transport (HSCT) fleet) on the chemistry of the stratosphere. An indication of a possible asymmetry between entrainment times characteristic for the Northern and Southern Hemispheres (with faster mixing from the north) would also impact HSCT assessment calculations, since most of the emissions would be expected in the northern midlatitudes. Faster transport of midlatitude air into the tropics also impacts the globally averaged lifetimes of longer-lived halogenated species, NO_y, N_2O, CH_4, etc., which directly influences assessments of stratospheric ozone depletion and global warming potentials.

Our results further suggest significantly larger concentrations of chlorine atoms in the lower tropical stratosphere than calculated using a photochemical model with standard gas-phase and heterogeneous chemistry. Chlorine atoms are the primary sink for several short-lived compounds (e.g., ethane and C_2Cl_4) and play a significant role in methane chemistry. Besides potential "missing" chemistry, such as heterogeneous chlorine activation on cirrus cloud particles [*Borrmann et al.*, 1996; *Solomon et al.*, 1997] that could be responsible for enhanced chlorine atom concentrations in the lower tropical stratosphere, our results point toward an important contribution of short-lived organic chlorine containing species to the Cl_y budget as has been suggested by *Ko et al.* [1997], *Schauffler et al.* [1999], and *Solomon et al.* [1994]. These compounds seem to be poorly represented by empirical relationships to estimate Cl_y from longer-lived tracer concentrations [e.g., *Woodbridge et al.*, 1995] that are presently used in many models of lower tropical stratospheric chemistry.

Acknowledgments. We thank Paul Wennberg, Tom Hanisco, and Eric Lanzendorf for the use of their OH radical data, Ru-Shan Gao and David Fahey for NO_y data, Jim Margitan for O_3 data, Jim Elkins for the use of the ASHOE/MAESA measurement data, and two anonymous reviewers for their very helpful comments. Thanks to Verity Stroud, Wilma Travnicek, and Bill Taylor for their support in the Lab at NCAR and Philip Mote for providing calculated entrainment timescales. Special thanks to the STRAT and POLARIS science team and the ER-2 and DC-8 ground crew and pilots, who made this study possible. We thank NASA for funding the STRAT and POLARIS missions. The National Center for Atmospheric Research is sponsored by the National Science Foundation. Part of this research was carried out by the Jet Propulsion Laboratory, California Institute of Technology, under a contract with the National Aeronautics and Space Administration.

References

Alternative Fluorocarbons Environmental Suitability Study, Production, sales and atmospheric release of fluorocarbons through 1995, AFEAS Admin. Organ. Washington, D C., 1997.

Andrews, D.G., J R. Holton, and C.B. Leovy, *Middle Atmosphere Dynamics*, 489 pp., Academic, San Diego, Calif., 1987.

Avallone, L M., and M.J. Prather, Photochemical evolution of ozone in the lower tropical stratosphere, *J. Geophys. Res*, *101*, 1457-1461, 1996.

Blake, D.R., N.J. Blake, T.W. Smith, O.W. Wingenter, and F.S. Rowland, Nonmethane hydrocarbon and halocarbon distributions during ASTEX/MAGE, June 1992, *J Geophys. Res.*, *101*, 4501-4510, 1996a.

Blake, N.J., D.R. Blake, B.C Sive, T Y. Chen, and F.S. Rowland, Biomass burning emissions and vertical distribution of atmospheric methyl halides and other reduced carbon gases in the South Atlantic region, *J. Geophys. Res.*, *101*, 24,151-24,164, 1996b.

Boering, K.A., J. B. C. Daube, S.C. Wofsy, M Loewenstein, J.R. Podolske, and E.R. Keim, Tracer-tracer-relationships and lower stratospheric dynamics: CO_2 and N_2O correlations during SPADE, *Geophys. Res. Lett.*, *21*, 2567-2570, 1994.

Boering, K.A., S.C Wofsy, J. B C. Daube, H.R. Schneider, M. Loewenstein, J.R. Podolske, and T.J Conway, Stratospheric mean ages and transport rates from observations of carbon dioxide and nitrous oxide, *Science*, *274*, 1340-1343, 1996.

Borrmann, S , S Solomon, J E. Dye, and B. Luo, The potential of cirrus clouds for heterogeneous chlorine activation, *Geophys. Res. Lett.*, *23*, 2133-2136, 1996

Daniel, J.S., S.M. Schauffler, W.H. Pollock, S Solomon, A. Weaver, L.E. Heidt, R.R Garcia, E.L. Atlas, and J.F. Vedder, On the age of stratospheric air and inorganic chlorine and bromine release, *J. Geophys. Res.*, *101* (D11), 16,757-16,770, 1996.

DeMore, W.B., S.P. Sander, C.J. Howard, A R. Ravishankara, D.M. Golden, C E. Kolb, R.F. Hampsen, M.J. Kurylo, and M.J. Molina, Chemical kinetics and photochemical data for use in stratospheric modeling: Evaluation No. 12, Jet Propul. Lab., Pasadena, Calif., 1997.

Dlugokencky, E.J., K.A. Masarie, P.M. Lang, and P.P. Tans, Continuing decline in the growth rate of the atmospheric methane burden, *Nature*, *393*, 447-450, 1998.

Elkins, J.W. et al., Airborne gas chromatograph for in-situ measurements of long-lived species in the upper troposphere and lower stratosphere, *Geophys. Res. Lett.*, *23* (4), 347-350, 1996.

Fahey, D W., C.S. Eubank, G. Hübler, and F.C. Fehsenfeld, Evaluation

of a catalytic reduction technique for the measurement of total reactive odd-nitrogen NO_y in the atmosphere, *J Atmos. Chem.*, *3*, 435-468, 1985.

Flocke, F., E. Atlas, S Madronich, S.M. Schauffler, K. Aikin, J.J. Margitan, and T.P. Bui, Observations of methyl nitrate in the lower stratosphere during STRAT: Implications for its gas phase production mechanisms, *Geophys. Res. Lett.*, *25*, 1891-1894, 1998.

Fraser, P.J., D.E Oram, C.E Reeves, S A Penkett, and A. McCulloch, Southern hemispheric halon trends (1978-1998) and global halon emissions, *J. Geophys. Res. 104*, 15985-16000, 1999.

Gao, R.S., et al., A comparison of observations and model simulations of NO_x/NO_y in the lower stratosphere, *Geophys. Res. Lett.*, *26*, 1153-1156, 1999

Goldan, P.D., W.C Kuster, D L. Albritton, and A L. Schmeltekopf, Stratospheric $CFCl_3$, CF_2Cl_2, and N_2O height profile measurements at several latitudes, *J Geophys. Res*, *85*, 413-423, 1980.

Goldan, P.D, W C Kuster, A L. Schmeltekopf, and F.C Fehsenfeld, Correction of atmospheric N_2O mixing ratio data, *J. Geophys. Res*, *86*, 5385-5386, 1981.

Grant, W.B, et al., Observations of reduced ozone concentrations in the tropical stratosphere after the eruption of Mt. Pinatubo, *Geophys Res Lett.*, *19*, 1109-1112, 1992

Hall, T.M, and D.W. Waugh, Tracer transport in the tropical stratosphere due to vertical diffusion and horizontal mixing, *Geophys. Res. Lett.*, *24*, 1383-1386, 1997.

Heidt, L.E., J.F Vedder, W.H. Pollock, and R.A. Lueb, Trace gases in the antarctic atmosphere, *J. Geophys. Res.*, *94*, 11,599-11,611, 1989.

Herman, R.L., et al, Tropical entrainment time scales inferred from stratospheric N_2O and CH_4 observations, *Geophys. Res. Lett.*, *25*, 2781-2784, 1998.

Herman, R.L., et al., Measurements of CO in the upper troposphere and lower stratosphere, *Chemosphere*, in press, 1999.

Hess, P.G., N. Srimani, and S.J. Flocke, Trajectories and related variations in the chemical composition of air for the Mauna Loa Observatory during 1991 and 1992, *J. Geophys. Res.*, *101*, 14,543-14,568, 1996.

Hoell, J.M., D.D Davis, D.J. Jacob, M.O. Rodgers, R.E. Newell, H.E. Fuelberg, R.J. McNeal, J.L. Raper, and R.J. Bendura, Pacific Exploratory Mission in the tropical Pacific: PEM-Tropics A, August-September 1996, *J. Geophys. Res.*, *104*, 5567-5583, 1999.

Hoffmann, D.J., J.T. Peterson, and R.M. Rosson, Climate Monitoring and Diagnostics Laboratory Summary Report No. 24, 166 pp. U.S. Dep. of Commer., Boulder, Colo., Dec. 1998.

Holton, J.R., P.H. Haynes, M.E. McIntyre, A.R. Douglass, R.B. Rood, and L Pfister, Stratosphere-troposphere exchange, *Rev Geophys.*, *33*, 403-439, 1995.

Hynes, A J., P.H. Wine, and A.R. Ravishankara, Kinetics of the OH + CO reaction under atmospheric conditions, *J. Geophys. Res*, *91*(D11), 11,815-11,820 1986.

Jaeglé, L., et al., Observed OH and HO_2 in the upper troposphere suggest a major source from convective injection of peroxides, *Geophys. Res. Lett.*, *24* (24), 3181-3184, 1997.

Keating, G.M., and D F. Young, Interim reference ozone models for the middle atmosphere, in *Handbook for MAP*, Vol. 16, edited by K. Labitzke, J.J. Barnett, and B. Edwards, pp. 205-229, Sci. Comm. on Solar-Terr. Phys. Secr., Univ. of Ill., Urbana, 1985.

Kinne, S., O.B. Toon, and M. J. Prather, Buffering of stratospheric circulation by changing amounts of tropical ozone: A Pinatubo case study, *Geophys. Res. Lett.*, *19*, 1927-1930, 1992.

Ko, M.K.W, N.D. Sze, C.J. Scott, and D.K. Weisenstein, On the relation between stratospheric chlorine/bromine loading and short-lived tropospheric trace gases, *J. Geophys. Res.*, *102*, 25,507-25,517, 1997.

May, R.D., and C.R. Webster, Data processing and calibration for tunable diode laser harmonic absorption spectrometers, *J. Quant. Spectrosc. Radiat. Transfer*, *49*, 335-347, 1993.

Michelsen, H.A, et al., Stratospheric chlorine partitioning: Constraints from shuttle-borne measurements of [HCl], [$ClNO_3$], and [ClO], *Geophys. Res. Lett.*, *23*, 2361-2364, 1996.

Michelsen, H.A., G.L. Manney, M.R. Gunson, C.P. Rinsland, and R. Zander, Correlations of stratospheric abundances of CH_4 and N_2O derived from ATMOS measurements, *Geophys. Res. Lett.*, *25*, 2777-2780, 1998.

Minschwaner, K., R.J. Salawitch, and M.B. McElroy, Absorption of solar radiation by O_2: Implications for O_3 and lifetimes of N_2O, $CFCl_3$ and CF_2Cl_2, *J. Geophys. Res.*, *98*, 10,543-10,561, 1993.

Minschwaner, K., A.E. Dessler, J.W. Elkins, C.M. Volk, D.W. Fahey, M. Loewenstein, J.R. Podolske, A.E. Roche, and K.R. Chan, Bulk properties of isentropic mixing into the tropics in the lower stratosphere, *J. Geophys. Res.*, *101*, 9433-9439, 1996.

Montzka, S.A., J.H. Butler, R.C. Myers, T.M Thompson, T.H. Swanson, A.D. Clarke, L.T. Lock, and J.W. Elkins, Decline in the tropospheric abundance of halogen from halocarbons: Implications for stratospheric ozone depletion, *Science*, *272*, 1318-1322, 1996.

Mote, P.W, K.H. Rosenlof, M.E. McIntyre, E.S. Carr, J.C. Gille, J R Holton, J.S. Kinnersley, H.C. Pumphrey, J.M. Russell III, and J.W. Waters, An atmospheric tape recorder: The imprint of tropical tropopause temperatures on stratospheric water vapor, *J. Geophys. Res.*, *101*, 3989-4006, 1996.

Mote, P.W., T J. Dunkerton, M E. McIntyre, E.A. Ray, P.H Haynes, and J.M. Russell III, Vertical velocity, vertical diffusion, and dilution by midlatitude air in the tropical lower stratosphere, *J Geophys. Res*, *103*, 8651-8666, 1998.

Murphy, D.M., D.W. Fahey, M.H Proffitt, S.C. Liu, K.R. Chan, C.S. Eubank, S R Kawa, and K.K. Kelly, Reactive nitrogen and its correlation with ozone in the lower stratosphere and upper troposphere, *J. Geophys Res.*, *98*, 8571-8573, 1993.

Nedoluha, G.E, D.E Siskind, J.T. Bachmeister, R M. Bevilacqua, and J.M.Russell III, Changes in upper stratospheric CH_4 and NO_2 as measured by HALOE and implications for changes in transport, *Geophys. Res. Lett.*, *25*, 987-990, 1998.

Newman, P.A., D.W. Fahey, W.H. Brune, M.J. Kurylo, and S.R. Kawa, Preface, *J. Geophys. Res.*, this issue.

Osterman, G.B., B. Sen, G.C. Toon, R.J. Salawitch, J.J. Margitan, J.-F. Blavier, D.W Fahey, and R.S. Gao, Partitioning of NO_y in the summer Arctic stratosphere, *Geophys. Res. Lett. 26*, 1157-1160, 1999.

Plumb, R.A., A "tropical pipe" model of stratospheric transport, *J Geophys. Res.*, *101*, 3957-3972, 1996.

Polvani, L.M., D.W. Waugh, and R.A. Plumb, On the subtropical edge of the stratospheric surf zone, *J. Atmos. Sci*, *52*, 1288-1309, 1995.

Proffitt, M.H., and R.J. McLaughlin, Fast-response dual-beam UV-absorption ozone photometer suitable for use on stratospheric balloons, *Rev. Sci. Instrum.*, *54*, 1719-1728, 1983.

Randel, W.J., J.C. Gille, A.E. Roche, J.B. Kumer, J.L. Mergenthaler, J.W. Waters, E.F Fishbein, and W.A. Lahoz, Stratospheric transport from the tropics to mid-latitudes by planetary-wave mixing, *Nature*, *365*, 533-535, 1993.

Randel, W.J., F. Wu, J.M. Russell III, and A Roche, Seasonal cycles and interannual variability in stratospheric CH_4 and H_2O observed in UARS Haloe data, *J. Atmos. Sci*, *55*, 163-185, 1998.

Roeth, E.P., R. Ruhnke, G. Moortgat, R. Meller, and W. Schneider, UV-VIS absorption cross sections and quantum yields for use in photochemistry and atmospheric modeling, 2, Organic substances, Forschungszentrum Juelich, Juelich, Germany, 1998.

Rosenlof, K.H., Seasonal cycle of the residual mean meridional circulation in the stratosphere, *J. Geophys. Res.*, *100*, 5173-5191, 1995.

Rosenlof, K.H., A.F. Tuck, K.K. Kelly, J.M. Russell III, and P.M. McCormick, Hemispheric asymmetries in water vapor and inferences about transport in the lower stratosphere, *J. Geophys. Res.*, *102*, 13,213-13,234, 1997.

Salawitch, R.J., et al., The diurnal variation of hydrogen, nitrogen, and chlorine radicals: Implications for the heterogeneous production of HNO_2, *Geophys. Res. Lett.*, *21*, 2551-2554, 1994.

Schauffler, S.M, E. Atlas, F. Flocke, R.A. Lueb, V. Stroud, and W. Travnicek, Measurements of bromine-containing organic compounds at the tropical tropopause, *Geophys. Res. Lett.*, *25* (3), 317-320, 1998.

Schauffler, S.M., E.L. Atlas, D.R. Blake, F. Flocke, X.X. Tie, R.A. Lueb, J.M. Lee-Taylor, V. Stroud, and W. Travnicek, Distributions of brominated organic compounds in the troposphere and lower stratosphere, *J Geophys. Res. 104*, 21513-21535, 1999.

Schoeberl, M.R., A.E. Roche, J.M. Russell III, D. Ortland, P.B. Hays, and J.W. Waters, An estimation of the dynamical isolation of the tropical lower stratosphere using UARS wind and trace gas observations of the quasi-biennial oscillation, *Geophys. Res. Lett.*, *24*, 53-56, 1997.

Scott, S.G., T P. Bui, K.R. Chan, and S.W. Bowen, The Meteorological Measurement System on the NASA ER-2 aircraft, *J. Atmos. Oceanic Technol.*, *7*, 525-540, 1990.

Sen, B., et al., The budget and partitioning of stratospheric chlorine during the 1997 Arctic summer, *J. Geophys. Res.*, this issue.

Singh, H.B., M. Kanakidou, P.J. Crutzen, and D.J. Jacob, High concentration and photochemical fate of oxygenated hydrocarbons in the global troposphere, *Nature*, *378*, 50-53, 1995.

Solomon, S., R R Garcia, and A.R. Ravishankara, On the role of iodine in ozone depletion, *J. Geophys. Res.*, *99*, 20,491-20,499, 1994.

Solomon, S., S Borrmann, R.R. Garcia, R. Portmann, L. Thomason, L.R Poole, D. Winker, and M.P McCormick, Heterogeneous chlorine chemistry in the tropopause region, *J. Geophys. Res.*, *102*, 21,411-21,429, 1997.

Stolarski, R , *1995 Scientific Assessment of the Atmospheric Effects of Stratospheric Aircraft*, Nat. Aeron. and Space Admin., Washington, D. C., 1995.

Travnicek, W., E.L. Atlas, F. Flocke, and S.M. Schauffler, Measurements of light halogenated tracers during POLARIS and comparison with a long-term record derived from archived tropospheric air samples, poster presented at the 1998 Conference on the Atmospheric Effects of Aviation, NASA Atmospheric Effects of Aviation Project, Virginia Beach, Va , April 25 - May 1, 1998.

Trepte, C.R , and M.H. Hitchman, Tropical stratospheric circulation deduced from satellite aerosol data, *Nature*, *355*, 626-628, 1992

Tuck, A F , et al., The Brewer-Dobson circulation in the light of high altitude *in situ* aircraft observations, *Q. J R Meteorol. Soc.*, *123*, 1-69, 1997a.

Tuck, A.F., W.H. Brune, and R.S Hipskind, Airborne Southern Hemisphere Ozone Experiment / Measurements for Assessing the Effects of Stratospheric Aircraft (ASHOE/MEASA): A road map, *J. Geophys Res.*, *102*, 3901-3904, 1997b.

Vedder, J.F., B.J. Tyson, R B. Brewer, C.A. Boitnott, and E C Y. Inn, Lower stratosphere measurements of variation with latitude of CF_2Cl_2, $CFCl_3$, CCl_4, and N_2O profiles in the northern hemisphere, *Geophys. Res. Lett.*, *5*, 33-36, 1978.

Vedder, J.F., E.C.Y. Inn, B.J. Tyson, C.A. Boitnott, and D. O'Hara, Measurements of CF_2Cl_2, $CFCl_3$, and N_2O in the lower stratosphere between 2°S and 73°N latitude, *J. Geophys Res.*, *86*, 7363-7368, 1981

Volk, C.M., et al., Quantifying transport between the tropical and mid-latitude lower stratosphere, *Science*, *272*, 1763-1768, 1996.

Waugh, D W., Seasonal variation of isentropic transport out of the tropical stratosphere, *J. Geophys. Res.*, *101*, 4007-4023, 1996

Webster, C R , R D. May, C A. Trimble, R.G. Chave, and J. Kendall, Aircraft (ER-2) laser infrared absorption spectrometer (ALIAS) for *in situ* stratospheric measurements of HCl, N_2O, CH_4, NO_2 and HNO_3, *Appl. Opt.*, *33*, 454-472, 1994.

Wennberg, P.O., R.C. Cohen, N.L. Hazen, L.B. Lapson, N.T Allen, T F. Hanisco, J.F. Oliver, N.W Lanham, J.N. Demusz, and J.G Anderson, Aircraft-borne, laser-induced fluorescence instrument for the *in situ* detection of hydroxyl and hydroperoxyl radicals, *Rev. Sci. Instrum.*, *65*, 1858-1876, 1994a.

Wennberg, P O., et al., Removal of stratospheric ozone by radicals· In situ measurements of OH, HO_2, NO, NO_2, ClO, and BrO, *Science*, *266*, 398-404, 1994b.

Wennberg, P O., et al., Hydrogen radicals, nitrogen radicals, and the production of ozone in the middle and upper troposphere, *Science*, *279*, 49-53, 1998

Wofsy, S C., K A. Boering, B.C. Daube, and M.B. McElroy, Vertical transport rates in the stratosphere in 1993 from observations of CO_2, N_2O and CH_4, *Geophys. Res. Lett.*, *21*, 2571-2574, 1994.

Woodbridge, E L., et al., Estimates of total organic and inorganic chlorine in the lower stratosphere from in situ and flask measurements during AASE II, *J. Geophys. Res* , *100*, 3057-3064, 1995.

E. Atlas, F Flocke, R A Lueb, and S M. Schauffler, NCAR Atmospheric Chemistry Division, P O. Box 3000, Boulder, CO 80307-3000. (ffl@ucar.edu)

D. R. Blake, Department of Chemistry, University of California at Irvine, Irvine, CA 92697

T. P. Bui, NASA Ames Research Center, Mail Stop 245-5, Moffett Field, CA 94035-1000

R. L. Herman, R. D. May, R. J. Salawitch, D C Scott, and C. R. Webster, NASA Jet Propulsion Laboratory, California Institute of Technology, 4800 Oak Grove Drive, Pasadena, CA 91109.

E. J. Moyer, Division of Geological and Planetary Sciences, California Institute of Technology, Pasadena, CA 91125.

K. H. Rosenlof, NOAA Aeronomy Laboratory, 325 Broadway, Boulder, CO 80303

(Received December 15, 1998; revised June 29, 1999;
accepted June 30, 1999.)